JVI Journals.ASM.org

Cullin4A and Cullin4B Are Interchangeable for HIV Vpr and Vpx Action through the CRL4 Ubiquitin Ligase Complex

Hamayun John Sharifi,[a] Andrea K. M. Furuya,[a] Robert M. Jellinger,[b] Michael D. Nekorchuk,[a] Carlos M. C. de Noronha[a]

Center for Immunology and Microbial Disease, Albany Medical College, Albany, New York, USA[a]; Division of HIV Medicine, Albany Medical Center, Albany, New York, USA[b]

ABSTRACT

Human immunodeficiency virus (HIV) seizes control of cellular cullin-RING E3 ubiquitin ligases (CRLs) to promote viral replication. HIV-1 Vpr and HIV-2/simian immunodeficiency virus (SIV) Vpr and Vpx engage the cullin4 (CUL4)-containing ubiquitin ligase complex (CRL4) to cause polyubiquitination and proteasomal degradation of host proteins, including ones that block infection. HIV-1 Vpr engages CRL4 to trigger the degradation of uracil-*N*-glycosylase 2 (UNG2). Both HIV-1 Vpr and HIV-2/SIV Vpr tap CRL4 to initiate G_2 cell cycle arrest. HIV-2/SIV Vpx secures CRL4 to degrade the antiviral protein SAMHD1. CRL4 includes either cullin4A (CUL4A) or cullin4B (CUL4B) among its components. Whether Vpr or Vpx relies on CUL4A, CUL4B, or both to act through CRL4 is not known. Reported structural, phenotypic, and intracellular distribution differences between the two CUL4 types led us to hypothesize that Vpr and Vpx employ these in a function-specific manner. Here we determined CUL4 requirements for HIV-1 and HIV-2/SIV Vpr-mediated G_2 cell cycle arrest, HIV-1 Vpr-mediated UNG2 degradation, and HIV-2 Vpx-mediated SAMHD1 degradation. Surprisingly, CUL4A and CUL4B are exchangeable for CRL4-dependent Vpr and Vpx action, except in primary macrophages, where Vpx relies on both CUL4A and CUL4B for maximal SAMHD1 depletion. This work highlights the need to consider both CUL4 types for Vpr and Vpx functions and also shows that the intracellular distribution of CUL4A and CUL4B can vary by cell type.

IMPORTANCE

The work presented here shows for the first time that HIV Vpr and Vpx do not rely exclusively on CUL4A to cause ubiquitination through the CRL4 ubiquitin ligase complex. Furthermore, our finding that intracellular CUL4 and SAMHD1 distributions can vary with cell type provides the basis for reconciling previous disparate findings regarding the site of SAMHD1 depletion. Finally, our observations with primary immune cells provide insight into the cell biology of CUL4A and CUL4B that will help differentiate the functions of these similar proteins.

Human immunodeficiency virus (HIV) infection remains a serious threat to human health. An understanding of the molecular biology underlying HIV replication and pathogenesis will be crucial for stopping this devastating pathogen. The molecular biology of HIV reflects the evolutionary interplay between virus and host. HIV infects primarily $CD4^+$ T cells and macrophages and must overcome intracellular restrictions to do so. HIV and simian immunodeficiency virus (SIV) commandeer cellular ubiquitin ligases to eliminate intrinsic antiviral proteins. The HIV protein Vif recruits the cellular cytidine deaminase APOBEC3G to the cullin5-elonginB/C complex (1). This interaction results in the polyubiquitination, and subsequent proteasome-dependent destruction, of APOBEC3G (2–6). In the absence of Vif, APOBEC3G is packaged into progeny virus, where, upon infection, it deaminates negative-DNA-strand cytidines during reverse transcription, thereby introducing G-to-A mutations into the coding strand. The hypermutated viral genome is thus rendered ineffective for the production of viral progeny (7–12). HIV-1 Vpu can tap the SCFβ-TrCP E3 ubiquitin ligase complex to help clear tetherin from the cell surface (13–15). In the absence of Vpu, tetherin links cellular and viral membranes to anchor virus to the host cell plasma membrane. Tetherin thus restricts viral dissemination (16–18).

HIV-1 Vpr and HIV-2/SIV Vpr and Vpx all act through the cullin4 (CUL4)-RING E3 ubiquitin ligase complex (CRL4). Vpx recruits SAMHD1, a cellular deoxynucleoside triphosphate triphosphohydrolase (19), to CRL4 to trigger its proteasome-dependent destruction (20–22). Elimination of SAMHD1 by Vpx allows cellular deoxynucleoside triphosphate (dNTP) levels to increase sufficiently to permit reverse transcription (23). HIV-1 and HIV-2/SIV Vpr expression triggers G_2 cell cycle arrest (24–30) through CRL4 complexes (31–36). Very recent work found HIV-1 Vpr to initiate G_2 arrest by the CRL4-dependent activation of the SLX4 complex (37). Whether HIV-2/SIV Vpr acts similarly remains to be determined. HIV-1 Vpr also boosts the turnover of uracil-*N*-glycosylase 2 (UNG2) and single-strand-selective monofunctional uracil DNA glycosylase (SMUG1) through the CRL4 complex (38–40). The impact of G_2 cell cycle arrest or UNG2 and SMUG1 degradation on HIV replication and pathogenesis remains unclear; however, G_2 arrest has been linked to immune evasion (37) and increased viral production (41) by HIV-1.

CRL4 complexes are defined by the inclusion of CUL4, a scaffold for the assembly of the E3 ubiquitin ligase. The carboxyl terminus of CUL4 engages ROC1, a ring-domain-containing protein which in turn binds and activates the E2 ligase. The E2 ligase is

Received 24 January 2014 **Accepted** 31 March 2014
Published ahead of print 9 April 2014
Editor: G. Silvestri
Address correspondence to Carlos M. C. de Noronha, deNoroC@mail.amc.edu.

doi:10.1128/JVI.00241-14

charged with and transfers ubiquitin to target proteins. The amino end of CUL4 secures the adaptor DNA damage binding protein 1 (DDB1), which recruits ubiquitination targets directly or indirectly through one of approximately 90 WD40-domain-containing proteins that confer substrate specificity to the complex (42–45). HIV-1 and HIV-2/SIV Vprs and HIV-2/SIV Vpx all engage the WD40 protein DCAF1 (also designated VprBP) to assemble with CRL4. DCAF1 and DDB1 are required for CRL4-dependent Vpr and Vpx functions (20, 31–33, 35, 37, 38, 40, 46–50).

Human cells encode two CUL4 types: types A and B. These CUL4 types share approximately 80% identity at the amino acid level, differing primarily at the amino terminus, where CUL4B is about 15% longer and carries a nuclear localization signal (NLS) (^{55}KKRK^{58}) (51). The gene for CUL4A is on chromosome 13 in humans, while that for CUL4B is on the X chromosome of all mammals tested. The CUL4 type required for Vpr and Vpx action has not been determined.

The amino acid sequence similarity between CUL4A and CUL4B suggests that the two proteins could be interchangeable, but this is not the case. No humans who lack functional CUL4A have been identified, likely due to a role in spermatogenesis similar to that observed for mice (52). Human males lacking functional CUL4B present with X-linked intellectual disability (XLID), while female carriers are unaffected (53–56). Nakagawa and Xiong showed previously that WDR5, an H3K4 methyltransferase, is specifically depleted by CUL4B, but not by CUL4A, and that this determines neuronal gene expression profiles (57). CUL4A overexpression has been associated with breast cancer (58), hepatocellular carcinoma (59), and pleural mesothelioma (60). A complementary observation showed that skin-specific deletion of CUL4A protected mice against UV-induced skin cancer (61).

Schröfelbauer et al. demonstrated previously that HIV-1 Vpr can be coisolated with CUL4A from lysates of cells overexpressing epitope-tagged versions of both proteins (39). CUL4B was not tested in those early experiments, leaving open the possibility that it could also assemble into complexes with Vpr and therefore mediate Vpr functions.

Based on the reported structural and subcellular distribution differences between CUL4A and CUL4B, we hypothesized that there are specific CUL4A and CUL4B requirements for different HIV phenotypes. Previous work showing that HIV-1 Vpr triggers G_2 cell cycle arrest by eliciting DNA damage signals (37, 62–66) led us to hypothesize that NLS-containing CUL4B is required for this function. Reports showing that SAMHD1 depletion is triggered in the nucleus (67–69) led us to posit that CUL4B is required for this phenotype as well. UNG2 can be found in both the cytoplasm and the nucleus (38), suggesting that HIV-1 Vpr-directed UNG2 degradation could be set off through CUL4A or CUL4B. In this work, we investigated the need for CUL4A and/or CUL4B for the Vpr and Vpx phenotypes that require the CRL4 ubiquitin ligase and show that the two CUL4 types are exchangeable for G_2 cell cycle arrest, UNG2 turnover, and SAMHD1 depletion. Furthermore, we show that in primary human monocyte-derived macrophages (hMDMs), both CUL4 types are required for optimal SAMHD1 depletion by Vpx. Finally, we demonstrate that the subcellular distributions of CUL4A and CUL4B can vary between cell types.

MATERIALS AND METHODS

Stably transduced cell lines. The following plasmids were used to generate lentiviral vectors for use in establishing stable cell lines: nontargeting (catalog no. RHS4743), CUL4A-specific (clone V2THS_32527), CUL4B-specific (clone V2THS_32515]), DCAF1/VprBP-specific (clone V2THS_74081), and DDB1-specific (clone V2THS_151130) pTRIPZ short hairpin RNA (shRNA) expression vectors for inducible transduction (Thermo Scientific Life Science Research) and firefly luciferase-specific shRNA (control shRNA) (pSicoRshluc was a gift from Tyler Jacks) (Addgene plasmid 14782), CUL4A-specific shRNA (catalog no. RHS4430-99165652, oligonucleotide V2LHS_32529; Thermo Scientific Life Science Research), and CUL4B-specific shRNA (catalog no. RHS4430-98475972, oligonucleotide V2LHS_32515; Thermo Scientific Life Science Research) for constitutive transduction. Of note, we blocked green fluorescent protein (GFP) expression in the constitutive CUL4A- and CUL4B-specific shRNA vectors by introducing a frameshift mutation into the *gfp* gene.

Five million HEK293T cells were transfected with an shRNA expression vector together with pLP1 (encodes Gag and Pol), pLP2 (encodes Rev), and pLP-VSV-G (encodes the vesicular stomatitis virus G protein [VSV-G]) (ViraPower Lentiviral Gateway Expression kit, catalog no. K496000; Invitrogen) at an equimolar ratio. Forty-eight hours after transfection, the cell supernatant was transferred into a 10-cm tissue-culture-treated petri plate containing 2.5 million HEK293T cells. Five hours after infection, fresh medium was applied. Forty-eight hours after infection, transduced HEK293T cells were selected by culturing in medium supplemented with 3 μg/ml puromycin. The puromycin-supplemented medium was replaced every 3 days until surviving cell populations expanded. Where specified, cell lines were induced to express shRNAs by incubation in medium containing doxycycline at a concentration of 0.5 μg/ml. Depletion of target proteins was confirmed by Western blotting.

Cell viability was determined by using Cell Counting kit 8 (Dojindo Molecular Technologies, Inc.) in accordance with the manufacturer's instructions. Treatment of cells with the translation inhibitor blasticidin at 10 μg/ml for 24 h was used as a positive control for cell killing.

Cell culture. HEK293T cells were maintained in Dulbecco's modified Eagle medium (DMEM) supplemented with 5% fetal bovine serum, 1 mM glutamine, 50 units/ml penicillin, and 50 μg/ml streptomycin. HEK293T stable lines were cultured in the same medium supplemented with 3 μg/ml puromycin.

Elutriated human monocytes were obtained from healthy donors at the University of Nebraska Medical Center (Omaha, NE). The monocytes were differentiated into macrophages by incubation in serum-free DMEM for 2 h, followed by a 12-day incubation in DMEM supplemented with 10% human AB serum. Peripheral blood lymphocytes (PBLs) were obtained by buffy coat isolation and cultured in DMEM supplemented with 10% human AB serum, 2.5 μg/ml phytohemagglutinin (PHA), and 10 units/ml interleukin 2 (IL-2) for 1 week to favor T-cell activation and expansion. The Albany Medical College Committee on Research Involving Human Subjects approved our protocol for the use of primary human leukocytes. A category 4 exemption from consent procedures was granted for the use of deidentified samples. All cultures were maintained at 37°C in the presence of 5% CO_2.

Immunoprecipitations. The HIV/SIV protein expression plasmids used in these assays were pcDNA3.1(−)HIV-1huVpr, pcDNA3.1(−)HIV-1FLAG-huVpr (31), pCMV-FLAG-SIV$_{mac239}$Vpr, and pCMV-FLAG-SIV$_{mac239}$Vpx. SIV$_{mac239}$Vpr and SIV$_{mac239}$Vpx were PCR amplified from SIV$_{mac239}$ and subcloned into the pCMV4 expression vector. Five million HEK293T cells were transfected with 20 μg of protein expression vector by using a standard calcium phosphate transfection protocol. Twenty-four hours after transfection, the cells were lysed with 1 ml of cold ELB buffer (50 mM HEPES [pH 7.3], 400 mM NaCl, 0.2% NP-40, 5 mM EDTA, 0.5 mM dithiothreitol [DTT], and protease inhibitor cocktail [catalog no. 11 836 153 001; Roche]). The lysates were clarified by centrifugation at 14,000 × *g* for 15 min at 4°C. The supernatants were then incubated with 25 μl of anti-FLAG M2 agarose resin (catalog no. A2220-5ML; Sigma-Aldrich) for 2 h at 4°C on a rotator. The anti-FLAG M2 beads were washed three times for 20 min in 1 ml of ELB buffer. Bound proteins were eluted by competition with 50 μl of 200 mg/ml FLAG peptide (catalog no.

F3290; Sigma-Aldrich) at 25°C for 30 min. An equal volume of 2× Laemmli buffer was added to each eluate. The samples were boiled for 10 min, resolved by SDS-PAGE, and analyzed for endogenous DCAF1, DDB1, CUL4A, CUL4B, SAMHD1, and UNG2 by Western blotting using specific antibodies as indicated (DCAF1 specific [catalog no. A301-887A; Bethyl Laboratories, Inc.], DDB1 specific [catalog no. 342300; Invitrogen], CUL4A specific [catalog no. 2699; Cell Signaling Technology], CUL4B specific [catalog no. C99995; Sigma-Aldrich], anti-SAMHD1 [catalog no. GTX83687; GeneTex[, and anti-UNG2 [a gift from Geir Slupphaug]). The FLAG epitope tag was detected by using anti-FLAG M2 (catalog no. F1804; Sigma-Aldrich).

Cell cycle and infectivity analyses. Cultures of HEK293T cells or HEK293T cell lines stably expressing shRNA (described above) were infected at a multiplicity of infection (MOI) of 3 with virus, as described below. Forty-eight hours after infection, the cells were collected and washed three times with 1 ml of phosphate-buffered saline (PBS). Cell nuclei were isolated by incubating the cell pellets in a solution containing 10 mM PIPES [piperazine-*N*,*N*′-bis(2-ethanesulfonic acid)], 0.1 M NaCl, 2 mM $MgCl_2$, and 0.1% Triton X-100 (pH 6.8). RNase A (0.2 mg/ml) and propidium iodide (0.02 mg/ml) were added to the suspended nuclei to degrade RNA and stain DNA, respectively. Nuclear DNA content was quantitated by flow cytometry using a FACSCanto flow cytometer (BD Biosciences). The fraction of cells in the G_1 or G_2/M phase of the cell cycle was determined by analysis using FlowJo software. For infectivity analyses, cells infected with a luciferase reporter virus were prepared for luciferase assays by using the Promega luciferase assay kit in accordance with the manufacturer's instructions (catalog no. E501; Promega). Photon emission was measured by using a Victor V3 luminometer (PerkinElmer).

Virus preparation. Five million HEK293T cells were cotransfected with expression vectors for either HIV-1 [pNL4-3*env*(−)*nef*(−)*gfp*(+)], HIV-1 lacking Vpr [pNL4-3*env*(−)*vpr*(−)*nef*(−)*gfp*(+)], HIV-2 [pGL-AN*nef*(−)*gfp*(+)], HIV-2 lacking Vpx [pGL-St*vpx*(−)*nef*(−)*gfp*(+)], HIV-2 lacking Vpr [pGL-Ec*vpr*(−)*nef*(−)*gfp*(+)], or HIV-2 lacking both Vpx and Vpr [pGL-St/Ec*vpr*(−)*nef*(−)*gfp*(+)] together with pCL-VSV-G for pseudotyping of HIV with the envelope glycoprotein of vesicular stomatitis virus. The HIV-1 clones were a gift from Vicente Planelles, and the HIV-2 clones originated as a gift from Mikako Fujita but have been modified to express GFP in place of Nef. The HIV-1 luciferase reporter clone [pNL4-3*env*(−)*nef*(−)*luc*(+)] was a gift from Nathaniel Landau. Transfections were done by using a standard calcium phosphate protocol with a total of 20 μg of DNA at an equimolar ratio of viral expression vector to VSV-G expression vector. VSV-G pseudotyping was used to promote efficient entry into all cell types used in this study. Twenty-four hours after transfection, the supernatant from infected cells was cleared of producer cells by centrifugation and then transferred to experimental cultures. Aliquots of supernatants obtained from viral producer cells were tested for the generation of equivalent viral titers by serial dilution and subsequent infection of the GHOST X4/R5 indicator cell line (from Vineet N. KewalRamani and Dan R. Littman through the NIH AIDS Research and Reference Reagent Program) (70).

Cell fractionations. Cells were separated into nuclear and cytosolic fractions as described previously but with minor modifications (71). Uninfected HEK293T cells, PBLs, or MDMs were collected and washed twice in PBS. The cells were incubated in 1 ml buffer B (10 mM HEPES [pH 7.9], 1.5 mM $MgCl_2$, 10 mM KCl, and protease inhibitor cocktail [catalog no. 11 836 153 001; Roche]) on ice for 10 min. Thirty microliters of 1% NP-40 was added as the samples were agitated. NP-40-treated samples were overlaid onto 1 ml of 1 M sucrose dissolved in buffer B. After centrifugation at 3,000 × *g* at 4°C for 10 min, 200 μl of supernatant was collected as the cytosolic fraction. The remaining supernatant was removed, and the pellet of nuclei was washed with, and then resuspended in, 1 ml of buffer B. Two-hundred microliters of nuclei in buffer B were collected as the nuclear fraction. An equal volume of 2× Laemmli buffer was added to the cytosolic and nuclear fractions. The cytoplasmic and nuclear lysates were heated to 94°C for 10 min before Western blot analysis. Samples were probed for histone H3 (anti-histone H3, catalog no. 9715; Cell Signaling Technology) and tubulin (antitubulin, catalog no. 3873S; Cell Signaling Technology) to confirm the purity of nuclear and cytoplasmic fractions, respectively. Tubulin or histone signals from fractionated samples were normalized to those of the whole-cell lysates to ensure an equal representation of the cytoplasm and nucleus.

siRNA transfection. The following short interfering RNAs (siRNAs) were obtained from Thermo Fisher Scientific Biosciences, Inc. (Dharmacon): nontargeting siRNA (catalog no. D-001210-02-50), CUL4A-specific siRNA (catalog no. L-012610-00-0020), CUL4B-specific siRNA (catalog no. L-017965-00-0020), and DCAF1-specific siRNA (catalog no. L-021119-01-0020). siRNA was transfected by using Lipofectamine 2000 (catalog no. 11668-019; Invitrogen) in accordance with the manufacturer's instructions.

Dominant negative CUL4 expression vectors. The dominant negative CUL4 (DNCUL4) expression constructs were generated by PCR amplification of the CUL4 cDNA sequence with primers that introduce additional residues to encode a hemagglutinin (HA) epitope tag at the 5′ end and a premature stop codon at the 3′ end. The resulting truncated proteins lack both the carboxy terminus necessary for ROC1 binding and the neddylation site. ROC1 is essential for E2 binding and, thus, the transfer of ubiquitin to target substrates. Neddylation is required to activate cullin ubiquitin ligase complexes. The primers used to generate the DNCUL4A construct were forward primer 5′-GCACTCTAGAACCATGGCCTACCCCTACGACGTGCCCGACTACGCCATGGCGGACGAGGCCCCG-3′ and reverse primer 5′-GTTTAAGCTTCACTGGGGTTAAGTGCACTTCC-3′. These primers amplified the first 545 amino acids of CUL4A. The DNA was inserted into the XbaI and HindIII sites of the pcDNA3.1(−) vector (catalog no. V795-20; Invitrogen/Life Science Technologies). The primers used to generate the DNCUL4B construct were forward primer 5′-GCACCTCGAGACCATGGCCTACCCCTACGACGTGCCCGACTACGCCATGATGTCACAGTCATCTGG-3′ and reverse primer 5′-GTACAAGCTTCACTGCTGCAAAAGAACC-3′, which amplified the first 493 amino acids of CUL4B. The DNA was inserted into the XhoI and HindIII sites of the pcDNA3.1(−) vector. The sources of the CUL4A and CUL4B cDNAs were pCMVFLAG-CUL4A and pCMVFLAG-CUL4B, respectively. Both FLAG-CUL4 constructs were gifts from Jianping Jin.

Other reagents used in this study. Anti-HA antibody (catalog no. 12CA5; Roche) was used for epitope tags, and anti-β-actin (catalog no. A5441; Sigma-Aldrich) and anti-CDC6 (catalog no. AHF0322; Invitrogen) antibodies were used for cellular proteins. For viral proteins, anti-HIV-1 p24 (catalog no. 183–H12-5C) was obtained from Bruce Chesebro and Hardy Chen through the NIH AIDS Research and Reference Reagent Program (72) (of note, this HIV-1 p24 antiserum is cross-reactive with HIV-2 p27), anti-HIV-1 Vpr (catalog no. 3951) was obtained from Jeffrey Kopp through the NIH AIDS Reagent Program, and anti-Vpx (catalog no. 2609) was obtained from Lee Ratner through the NIH AIDS Reagent Program (73). For plasmids, the LaminC-eGFP (enhanced green fluorescent protein) construct was a gift from Ronald Goldman, and the pcDNA3.1(−)HIV-2FLAG-huVpr and UNG2-2HA expression constructs were generated as described previously (31, 38). The neddylation inhibitor MLN4924 was a gift from Millennium Pharmaceuticals.

Densitometric analysis. All densitometric analyses were done by using ImageJ image analysis software from the NIH (http://rsbweb.nih.gov/ij/). All chemiluminescent imaging was done by using an Alpha Innotech FluorChem HD2 imaging system.

Statistical analysis. The two-tailed Student *t* test was used to determine statistical significance.

RESULTS

HIV-1 Vpr can trigger G_2 cell cycle arrest in the absence of either CUL4A or CUL4B but not both. In order to test whether HIV-1 Vpr specifically requires CUL4A, CUL4B, or both together to trigger G_2 cell cycle arrest, we generated HEK293T cell lines that stably

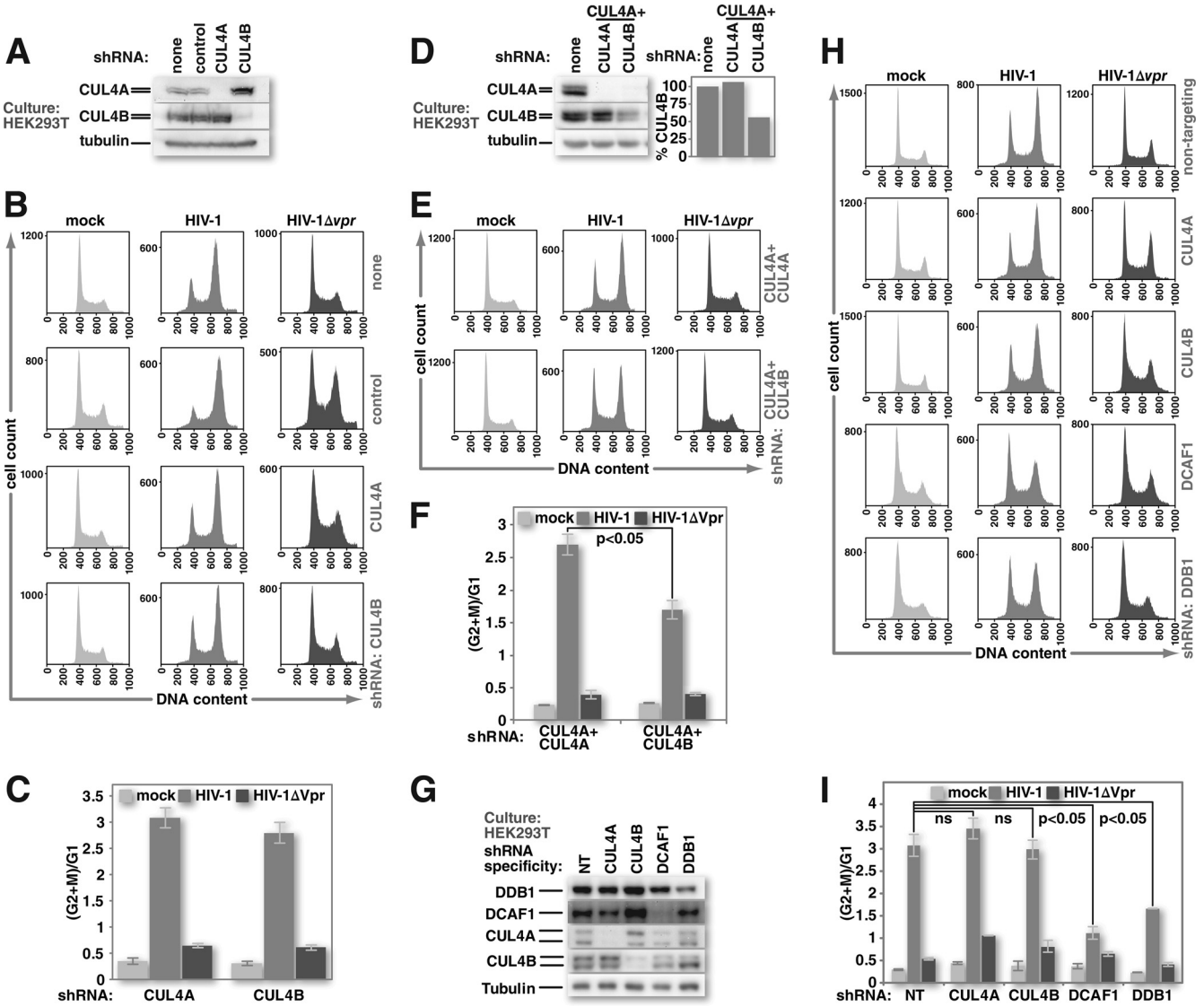

FIG 1 HIV-1 Vpr can trigger G_2 cell cycle arrest in the absence of either CUL4A or CUL4B but not both. (A) Cultures of HEK293T cells or HEK293T cells that stably express shRNA against firefly luciferase (control), CUL4A, or CUL4B were tested for CUL4-specific protein depletion by Western blotting. (B) HEK293T and HEK293T stably shRNA-expressing cell lines were mock infected or infected with HIV-1 or HIV-1 lacking Vpr at equivalent MOIs. Forty-eight hours after infection, cell nuclei were harvested, treated with RNase A and propidium iodide, and analyzed for DNA content by flow cytometry. (C) The ratio of nuclei with 4N DNA content (G2+M) to those with 2N DNA content (G1) was determined by using FlowJo software for replicates of the experiment shown in panel B. (D) HEK293T cells that stably express CUL4A-specific shRNA were depleted of CUL4B by transduction of a CUL4B-specific lentiviral expression vector. Transduction with a vector for CUL4A-specific shRNA was used as a control. Cultures under each experimental condition were tested for specific CUL4 protein depletion by Western blotting. (E) The HEK293T cultures described above for panel D were either mock infected or infected with HIV-1 or HIV-1 lacking Vpr. Nuclei from these cells were harvested 48 h after infection and analyzed for DNA content by flow cytometry, as described above for panel B. (F) The ratio of nuclei from HEK293T cells, as described above for panels D and E, with 4N DNA content to those with 2N DNA content was calculated and graphed as described above for panel C. (G) HEK293T cells with stably integrated lentiviral vectors that encode doxycycline-inducible shRNAs specific for CRL4 components were induced to express their respective shRNAs for 5 days. Transient depletion of target proteins was confirmed by Western blotting. Expression of a nontargeting (NT) shRNA served as a control. (H) HEK293T cells, as described above for panel G, were either mock infected or infected with HIV-1 or HIV-1 lacking Vpr. Forty-eight hours after infection, nuclei were isolated from these cells, and DNA content was assessed by using flow cytometry as described above for panels B and E. (I) The ratios of 4N to 2N DNA-containing nuclei, from the experiments described above for panels G and H, were calculated and graphed as described above for panels C and F ($n = 3$). All error bars show standard deviations. The two-tailed Student t test was used to determine statistical significance.

express shRNA directed against either CUL4A or CUL4B. These cell lines replicate with kinetics equivalent to those of parental populations but produce little or no detectable CUL4 corresponding to the targeted species (Fig. 1A). HEK293T cells stably expressing shRNA directed against firefly luciferase served as our nontargeting control because firefly luciferase is not expressed in mammalian cells. HEK293T cells are an established cell line for studying HIV replication. Although HEK293T cells lack the CD4 receptor necessary for HIV entry, pseudotyping of the virus with the glycoprotein of vesicular stomatitis virus (VSV-G) enables efficient entry into these cells (74). VSV-G-pseudotyped HIV replicates well in permissive cell lines such as HEK293T cells (75).

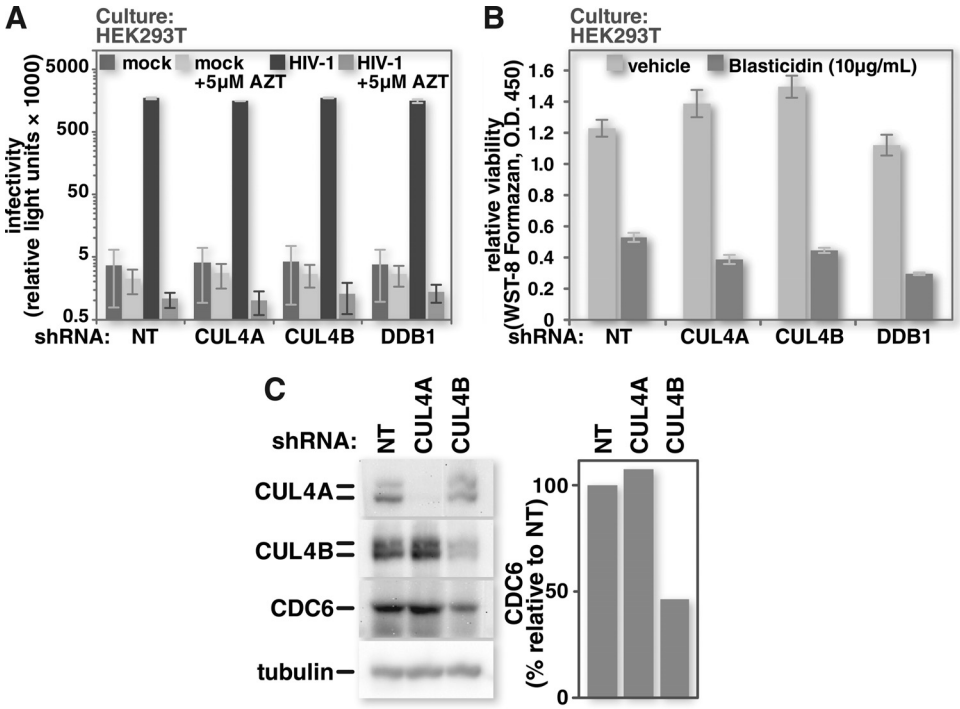

FIG 2 CRL4 depletion does not impair HIV-1 infectivity or viability of HEK293T cells. (A) HEK293T cells with stably integrated doxycycline-inducible cassettes for the expression of either a nontargeting shRNA or ones specific for CRL4 component mRNAs were induced with doxycycline. Five days after the start of induction, the cells were either mock infected or infected with VSV-G-pseudotyped HIV-1 encoding firefly luciferase in place of *nef*. Forty-eight hours after infection, the cells were harvested, and luciferase activity was measured by photon emission under each condition. Pretreatment of cultures with 5 μM the reverse transcription inhibitor zidovudine (AZT) served as a control to demonstrate impaired infectivity. (B) HEK293T cells were depleted of CRL4 components as described above for panel A. CRL4-depleted HEK293T cell viability was assessed by measuring water-soluble tetrazolium salt (WST-8) formazan reagent cleavage by cellular dehydrogenases. Pretreatment of cells with 10 μg/ml of the eukaryotic toxin blasticidin served as a control to demonstrate loss of viability. O.D., optical density. (C) HEK293T cells were depleted of CUL4A or CUL4B by induction of specific shRNAs. At 3 days postinduction, the cells were harvested and lysed. Cell lysates were resolved by SDS-PAGE, and Western blots were probed for CUL4A, CUL4B, CDC6, and tubulin. ($n = 3$ for panels A and B.) All error bars show standard deviations. The two-tailed Student *t* test was used to determine statistical significance.

HEK293T cells, whether depleted of CUL4A or CUL4B, were arrested in response to infection with HIV-1 expressing Vpr but not after infection with a virus lacking the capacity to express Vpr (Fig. 1B and C). To demonstrate the requirement for at least one CUL4 type, we simultaneously depleted both CUL4A and CUL4B and monitored HIV-1 Vpr-mediated G_2 cell cycle arrest. Here we transduced HEK293T cells that stably express CUL4A-specific shRNA with a lentiviral vector encoding CUL4B-specific shRNA. To ensure that our results were due to a reduction of CUL4B levels and not due to either lentiviral vector transduction or transient shRNA expression, we transduced another set of cultures with a lentiviral vector encoding the same CUL4A-specific shRNA. This procedure partially eliminated the residual CUL4 type (Fig. 1D). As expected, depletion of both CUL4A and CUL4B reduced HIV-1 Vpr-mediated G_2 cell cycle arrest (Fig. 1E and F). Importantly, the reduction in G_2 arrest was proportional to the depletion of the remaining CUL4 type.

In order to rule out the possibility that constitutive expression of CUL4-specific shRNA, prolonged antibiotic selection, or both selected for the expansion of cell populations in which the remaining CUL4 type can compensate for the depleted CUL4 type, we generated HEK293T lines that carry a doxycycline-inducible cassette for the expression of shRNA specific for CUL4A or CUL4B mRNA. HEK293T cells with inducible nontargeting shRNA served as a negative control, while cells with shRNAs against either DCAF1 or DDB1 mRNA served as positive controls. The results were similar to those observed for the constitutive shRNA-expressing cell lines. Transient depletion of CUL4A or CUL4B alone did not impair HIV-1 Vpr-mediated G_2 arrest. Depletion of either DCAF1 or DDB1, however, did block Vpr-mediated arrest (Fig. 1H and I). Of note, the depletion of DDB1 was relatively modest compared to the depletion obtained for either CUL4A or CUL4B (Fig. 1G). This weaker depletion, however, had a greater impact on HIV-1 Vpr-mediated G_2 arrest than that of either CUL4 type alone. Because DDB1 functions as the linker to recruit substrate specificity adaptors for both CUL4A and CUL4B, depletion of DDB1 simultaneously blocks the activity of both CUL4 types. Thus, HIV-1 Vpr can mediate G_2 cell cycle arrest through either CUL4A or CUL4B as long as the function of at least one of the two CUL4 types is maintained.

CRL4 depletion does not impair HIV-1 infectivity or the viability of HEK293T cells. Vpr is dispensable for efficient HIV infection in many cell types, including HEK293T cells (76, 77). This led us to hypothesize that the CRL4 components with which Vpr associates are also dispensable for infection of these cells. Using VSV-G-pseudotyped HIV-1 that encodes firefly luciferase as a reporter in place of *nef*, we infected cells depleted of CRL4 complex components at matched MOIs and, as expected, observed no impairment of infectivity (Fig. 2A). Furthermore, CRL4 depletion did not reduce cell viability (Fig. 2B).

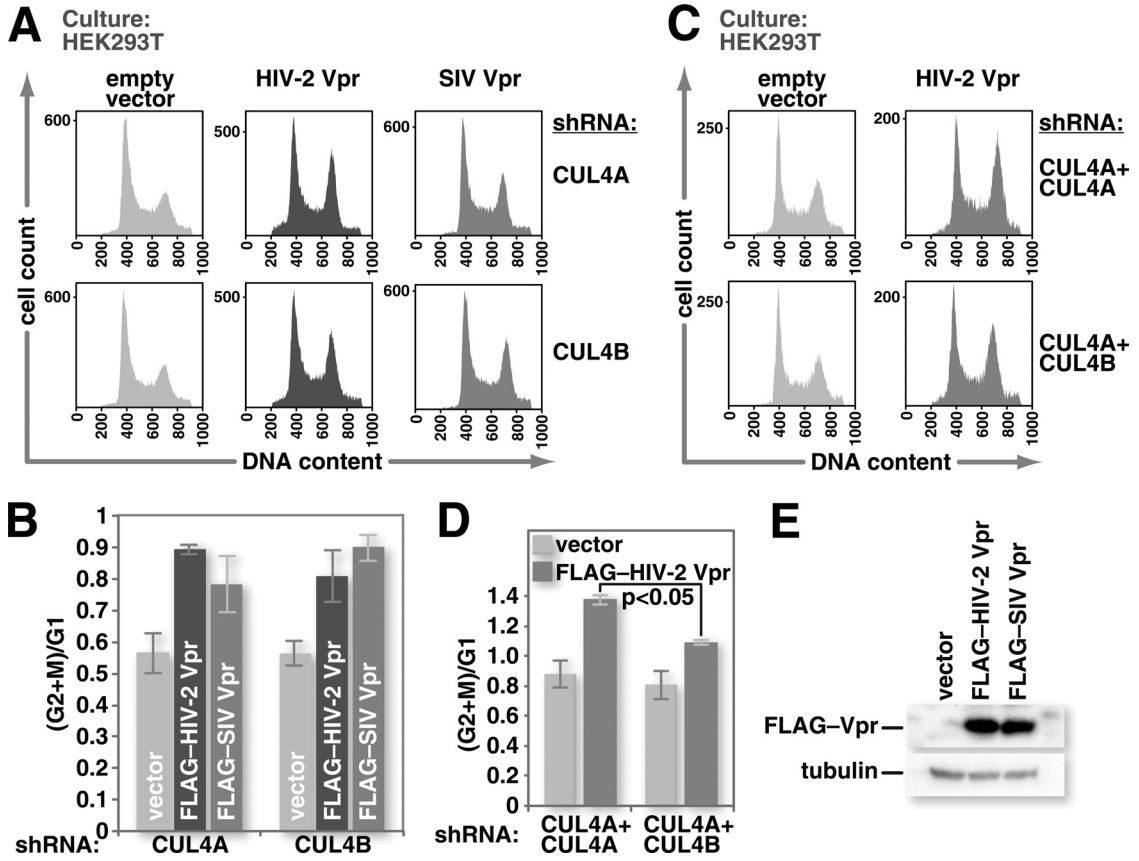

FIG 3 HIV-2/SIV$_{mac239}$ Vpr can trigger G_2 cell cycle arrest through either CUL4A or CUL4B. (A) HEK293T cells stably expressing shRNA specific for either CUL4A or CUL4B mRNA were transfected with either an empty expression vector or one for FLAG–HIV-2 Vpr or FLAG-SIV$_{mac239}$ Vpr and a small amount (7.5% of the total DNA) of an expression vector for LaminC-eGFP. Forty-eight hours after transfection, the cultures were harvested, and cell nuclei were isolated. Nuclei were treated with RNase A and stained with propidium iodide. Flow cytometry was used for gating on transfected (LaminC-eGFP-positive) cell nuclei, and DNA content was determined by measuring propidium iodide fluorescence intensity. (B) HEK293T cells that stably express shRNA specific for CUL4A were depleted of CUL4B as described in the legend of Fig. 1D. These cells were then transfected with either an empty expression vector or one for FLAG–HIV-2 Vpr. Flow cytometry was used to identify nuclei from transfected cells and to assess their DNA content as described above for panel A. (C and D) Ratios of nuclei with 4N DNA content (G2+M) to those with 2N DNA content (G1) were determined by using FlowJo software for replicates of the experiments shown in panels A (C) and B (D). (E) An empty expression vector or one for FLAG–HIV-2 Vpr or FLAG-SIV$_{mac239}$ Vpr was transfected into HEK293T cells. Twenty-four hours after transfection, the cells were harvested, and expression of FLAG-tagged Vpr was confirmed by Western blot analysis with FLAG-specific antibody ($n = 3$). All error bars show standard deviations. The two-tailed Student t test was used to determine statistical significance.

The similarity in Vpr-mediated G_2 cell cycle arrest profiles after depletion of CUL4A or CUL4B prompted us to confirm that we could distinguish between CUL4A- and CUL4B-specific effects in our system. Zou et al. demonstrated previously that the replication licensing factor CDC6 is positively regulated by CUL4B but not by CUL4A (78). We therefore induced the expression of CUL4A- or CUL4B-specific shRNA in cells that were stably transduced with the respective expression constructs. As in the previous work, cells depleted of CUL4B, but not those depleted of CUL4A, expressed lower levels of CDC6 (Fig. 2C). In summary, in our HEK293T system, depletion of CUL4A or CUL4B did not impact HIV-1 infectivity or cell viability. Furthermore, while Vpr-mediated G_2 cell cycle arrest proceeded in the absence of either CUL4A or CUL4B, the CUL4B-specific impact on CDC6 was preserved.

HIV-2/SIV$_{mac239}$ Vpr can trigger G_2 cell cycle arrest through either CUL4A or CUL4B. HIV-2 and some SIVs encode two HIV-1 Vpr-like proteins: Vpr and Vpx. HIV-2/SIV Vpr, like HIV-1 Vpr, can trigger G_2 cell cycle arrest through the CRL4 complex. We previously observed a smaller percentage of arrested cells upon the expression of HIV-2 Vpr than upon the expression of HIV-1 Vpr when equivalent quantities of expression vectors for the proteins were transfected into HEK293T cells (31). This may be attributable to lower levels of HIV-2/SIV Vpr (79) but may also be due to a requirement for a specific CUL4 type. Thus, whereas HIV-1 Vpr can use any CUL4 type with which it assembles to enable G_2 cell cycle arrest, HIV-2/SIV Vpr may depend on one CUL4 type. This could reduce the efficiency with which HIV-2/SIV Vpr promotes cell cycle arrest relative to that of HIV-1 Vpr. To test this, we transfected HEK293T cells that stably express shRNA against either CUL4A or CUL4B with an expression vector for FLAG-epitope-tagged HIV-2 Vpr or SIV Vpr and investigated the capacity of these Vprs to promote G_2 cell cycle arrest. The SIV Vpr protein that we used in these experiments was derived from the rhesus macaque 239 clone of SIV and is similar to HIV-2 Vpr in both sequence and function. Both the FLAG-epitope-tagged HIV-2 Vpr and SIV Vpr constructs led to robust expression of their respective viral proteins (Fig. 3E). Empty vector transfection

served as a control to demonstrate that DNA transfection does not alter the cell cycle progression of these cells. Expression of either FLAG–HIV-2 Vpr or FLAG-SIV Vpr caused an accumulation of cells in G_2 regardless of whether CUL4A or CUL4B was depleted (Fig. 3A and C). To investigate whether at least one CUL4 type is required for HIV-2 Vpr-mediated cell cycle arrest, we simultaneously depleted HEK293T cells of CUL4A and CUL4B, as described above (Fig. 1D). We then transfected these cells with an expression vector for FLAG–HIV-2 Vpr to assess the capacity of HIV-2 Vpr to promote cell cycle arrest under these conditions. As with HIV-1 Vpr, the simultaneous depletion of both CUL4A and CUL4B impaired HIV-2 Vpr-induced G_2 cell cycle arrest (Fig. 3B and D). Thus, like HIV-1 Vpr, HIV-2/SIV Vpr can trigger cell cycle arrest through either CUL4A- or CUL4B-containing CRL4 complexes.

HIV-1 Vpr-mediated UNG2 degradation and constitutive UNG2 turnover are not specifically dependent on CUL4A or CUL4B. UNG2 does not impact Vpr-mediated G_2 cell cycle arrest (80, 81), and the role of UNG2 in HIV infection remains unclear. Work from several laboratories showed that UNG2 has a positive impact on HIV-1 (39, 82, 83). In contrast, some laboratories found that UNG2 hinders HIV-1 (84, 85), whereas others found UNG2 to have no measurable impact on the virus (7, 86). Interestingly, one work linked the requirement for UNG2 to coreceptor usage (83). Despite the ambiguity surrounding the role of UNG2 in HIV infection, its connection with Vpr is well established. Vpr assembles with UNG2 (87–89) (see Fig. 5), and the expression of HIV-1 Vpr markedly reduces the levels of UNG2. HIV-1 Vpr-mediated UNG2 depletion can occur through degradation via the CRL4 complex (38, 40, 90) but is also impacted at the level of transcription from its native promoter (81, 91). To focus exclusively on CRL4-dependent Vpr-mediated degradation of UNG2, we produced UNG2 from a transfected plasmid under the control of a cytomegalovirus immediate early (CMV-IE) promoter and determined the contribution of CUL4A and CUL4B to its Vpr-enhanced turnover. To test whether HIV-1 Vpr can boost CRL4-mediated UNG2 degradation in the context of an infection, we again used constitutive CUL4-specific shRNA-expressing HEK293T cells. These cultures were transfected with the UNG2-2HA expression vector 24 h prior to infection with HIV-1 or HIV-1 lacking the capacity to express Vpr. Cells were harvested 48 h after infection, and whole-cell lysates were probed for UNG2-2HA levels by Western blotting. UNG2-2HA was depleted in cells infected with HIV-1 that can express Vpr but not in uninfected cells or in cells infected with HIV-1 lacking Vpr. UNG2-2HA depletion in the presence of HIV-1 Vpr occurred in both cells depleted of CUL4A and cells depleted of CUL4B. In each CUL4-specific shRNA-expressing cell line, the coexpression of UNG2-2HA with a dominant negative version of the abundant CUL4 type (DNCUL4) prevented UNG2-2HA degradation in the presence of Vpr (Fig. 4A). These CUL4 mutants lack carboxyl termini and thus cannot be neddylated, engage ROC1, or, by extension, assemble with the E2 ligase. The expressed amino-terminal portion of both dominant negative CUL4 proteins engages DDB1 (42) and therefore should compete with endogenous CUL4 for DDB1 binding (92). These data demonstrate that, like G_2 cell cycle arrest, HIV-1 Vpr-mediated UNG2 degradation does not rely on a single CUL4 species. Of note, coexpression of DNCUL4 led to increased steady-state UNG2-2HA levels under all conditions, including in uninfected cells. We have previously shown that UNG2 is normally turned over by the CRL4 complex in a DCAF1-dependent manner and that HIV-1 Vpr expression enhances this constitutive turnover (38). The increase in steady-state levels of UNG2-2HA in the presence of DNCUL4 was not sufficient to explain the observed preservation from HIV-1 Vpr-mediated degradation, as no decline in the overall levels of UNG2-2HA was observed when we compared uninfected cells, infected cells, and cells infected with virus lacking Vpr. The increase in steady-state UNG2-2HA levels upon the expression of a dominant negative version of the abundant CUL4 type suggests that constitutive UNG2 turnover by CRL4 could be mediated by either CUL4A or CUL4B. To further test this, we transfected HEK293T cells, transiently depleted of CRL4 components by doxycycline-induced shRNA expression, with the UNG2-2HA expression vector. Seventy-two hours after transfection, the cells were harvested, and the levels of UNG2-2HA were assessed by Western blotting. UNG2-2HA levels remained consistent in HEK293T cells expressing nontargeting or CUL4A- or CUL4B-specific shRNAs but increased in cells expressing shRNA against DCAF1 or DDB1 (Fig. 4B). These data indicate that constitutive turnover of UNG2 by CRL4 also does not rely on a specific CUL4 type.

CUL4A and CUL4B are both coisolated with Vpr and Vpx. HIV-1 Vpr and HIV-2/SIV Vpr and Vpx all act through the CRL4 ubiquitin ligase complex. CUL4A and CUL4B were interchangeable for the HIV-1 Vpr and HIV-2/SIV Vpr phenotypes that we tested. HIV-2/SIV Vpr and Vpx are structurally similar to HIV-1 Vpr but do not necessarily deplete the same targets. Specifically, HIV-1 Vpr triggers UNG2 depletion; however, neither HIV-2/SIV_{mac239} Vpr nor Vpx shares this phenotype. Conversely, HIV-2/SIV_{mac239} Vpx mediates the depletion of SAMDH1, but HIV-1 Vpr and HIV-2/SIV_{mac239} Vpr do not (see Fig. 6A). These observations prompted us to ask whether differences between Vpr and Vpx functions are linked to differential associations with CUL4A- or CUL4B-containing CRL4 complexes.

To determine the composition of the CRL4 complexes that are associated with Vpr and Vpx, we transfected HEK293T cells with expression vectors encoding FLAG-epitope-tagged versions of HIV-1 Vpr, SIV_{mac239} Vpr, or SIV_{mac239} Vpx. Twenty-four hours after transfection, the cells were lysed, and epitope-tagged proteins were isolated with FLAG-specific antibody conjugated to agarose beads. The antibody-bound proteins were eluted by competition with FLAG peptide. The eluate was analyzed for endogenous CRL4 complex components by Western blotting with the corresponding antisera. We isolated CRL4 complexes with all three viral proteins as well as their respective cellular targets (Fig. 5).

Interestingly, lower levels of CRL4 complex components were coisolated with Vpx, with the exception of CUL4B. This suggested that CUL4B may be key for Vpx function. Input sample blots all showed equivalent quantities of CUL4A and CUL4B, ruling out the possibility that Vpx expression either boosts that of CUL4B or hinders that of CUL4A. Thus, either Vpx-containing CRL4 complexes have a greater affinity for CUL4B or they reside in compartments where CUL4B is more abundant. This observation is consistent with reports that SAMHD1 is degraded in the nucleus, where CUL4B has been reported to reside, and led us to hypothesize that Vpx triggers SAMHD1 depletion more efficiently in cells expressing CUL4B.

Vpx can initiate SAMHD1 depletion through either CUL4A- or CUL4B-containing CRL4 complexes, but both CUL4 types are required for maximal SAMHD1 depletion in primary macrophages. The coimmunoprecipitation results led us to ask

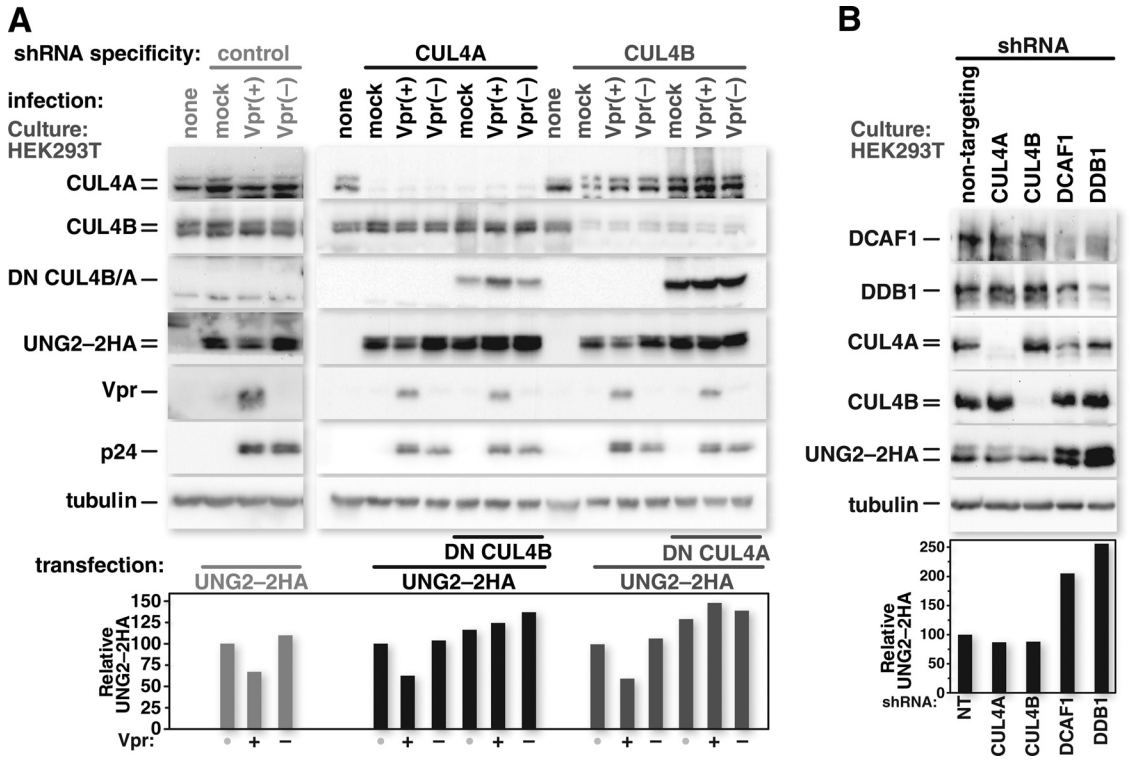

FIG 4 HIV-1 Vpr-mediated UNG2 degradation and constitutive UNG2 turnover are not specifically dependent on CUL4A or CUL4B. (A) HEK293T cells that stably express a control shRNA were transfected with an expression vector for UNG2-2HA. HEK293T cells that stably express shRNA targeting CUL4A or CUL4B mRNA were transfected with an expression vector for UNG2-2HA together with either an empty expression vector or one for an HA-tagged dominant negative version of the abundant CUL4 type. Twenty-four hours after transfection, the cells were mock infected or infected with HIV-1 or HIV-1 lacking Vpr. Forty-eight hours after infection, the cells were harvested and lysed. Cell lysates were resolved by SDS-PAGE and probed for CUL4A, CUL4B, tubulin, the HA epitope, HIV-1 p24, and HIV-1 Vpr by Western blotting using the corresponding antibodies. (B) HEK293T cells stably carrying doxycycline-inducible shRNA cassettes specific for CRL4 components were induced to express their respective shRNAs for 5 days. CRL4-depleted HEK293T cells were then transfected with the UNG2-2HA expression vector and harvested 72 h after transfection. Cell lysates were resolved by SDS-PAGE, and Western blots were probed for specific CRL4 components and the HA epitope by using the corresponding antibodies. Densitometric measurements performed on the UNG2-2HA bands were normalized to the values of the respective tubulin bands. The relative intensities of the UNG2-2HA bands were graphed based on the values obtained from the densitometric analysis.

whether CUL4A and CUL4B are interchangeable for Vpx-mediated depletion of SAMHD1. We again used stable, constitutive, shRNA-expressing HEK293T cell lines. These cells were either mock infected or infected with HIV-1 or HIV-2. Viruses lacking the capacity to express Vpr or Vpx served as negative controls to link these gene products with their respective protein depletion phenotypes. Twenty-four hours after infection, cells were harvested, and the protein content of whole-cell lysates was evaluated by Western blot analysis. Infection with HIV-2 encoding Vpx caused a marked depletion of SAMHD1 in cells that express both CUL4 types, CUL4A alone, or CUL4B alone. Of note, the interchangeability of CUL4 types for HIV-1 Vpr-mediated UNG2 depletion was recapitulated here, although we cannot rule out a possible transcriptional effect on endogenous UNG2 expression in this experiment (Fig. 6A).

The requirement for CUL4A and CUL4B for Vpx-mediated SAMHD1 degradation was also tested in primary hMDMs. This offered a number of important experimental differences. Unlike HEK293T cells, these cells are nondividing, terminally differentiated, primary cells that serve as HIV infection targets *in vivo*. Additionally, although SAMHD1 is expressed in HEK293T cells, it does not have the potent anti-HIV effect that it does in macrophages (23, 93). Furthermore, because these cells are nondividing primary cells that are difficult to infect efficiently with retroviral vectors, we targeted the mRNA of CUL4A, CUL4B, both CUL4A and CUL4B, or DCAF1 with specific siRNAs (Fig. 6B). The cultures were subsequently infected with HIV-2 at a high multiplicity of infection (MOI = 10). Infection with HIV-2 carrying Vpx triggered efficient depletion of endogenous SAMHD1 in cells transfected with nontargeting siRNA. Of note, the cultures were harvested <24 h after infection so that depletion would be due mostly if not exclusively to Vpx carried in the virion rather than that expressed from proviruses. Marked, albeit incomplete, SAMHD1 depletion was observed after siRNA-mediated removal of CUL4A or CUL4B. The removal of CUL4A and CUL4B together, however, substantially blocked the depletion of SAMHD1, resulting in a phenotype similar to that observed after DCAF1 depletion (Fig. 6C). These results demonstrate that CUL4A and CUL4B are interchangeable for Vpx-mediated depletion of SAMHD1, but neither CUL4 type alone was sufficient for complete SAMHD1 depletion in primary hMDMs.

Intracellular CUL4A and CUL4B distributions vary by cell type. The interchangeability of CUL4A and CUL4B for Vpr and Vpx phenotypes prompted us to examine the intracellular distribution of CRL4 components. Cytoplasmic and nuclear fractions were isolated and probed for CRL4 constituents. In HEK293T

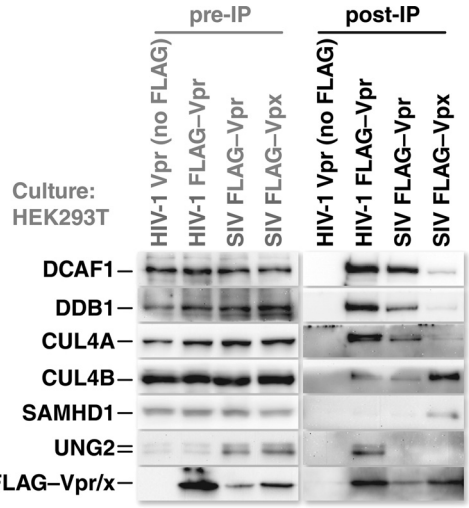

FIG 5 CUL4A and CUL4B are both coisolated with Vpr and Vpx. Cultures of HEK293T cells were transfected with expression vectors for untagged HIV-1 Vpr or FLAG-epitope-tagged HIV-1 Vpr, SIV Vpr, or SIV Vpx. Twenty-four hours after transfection, the cells were lysed, and insoluble debris was removed by centrifugation. Cleared lysates were incubated with FLAG-specific-antibody-coated beads to isolate the epitope-tagged viral proteins. The isolated viral proteins were subsequently eluted from the beads by competition with FLAG peptide. Proteins present in the eluates were resolved by SDS-PAGE and identified by Western blotting with specific antibodies. Preimmunoprecipitation (pre-IP) samples were derived from the lysates prior to incubation with antibody-coated beads. Untagged HIV-1 Vpr served as a control to ensure that the identified proteins were isolated through interactions with tagged viral proteins rather than nonspecific interactions with the antibody-coated beads.

cells, CRL4 complex components, including CUL4B, were abundant in the cytoplasm (Fig. 7A, left). However, HEK293T cells are not natural targets of HIV infection. We thus determined whether primary T cells exhibit a similar distribution of CRL4 components. Primary human T cells displayed a CRL4 component distribution profile similar to that of HEK293T cells, with both CUL4A and CUL4B being abundant in the cytosol (Fig. 7A, middle). Interestingly, the CUL4 detected in the nucleus consisted of a single higher-molecular-weight band. This was true for both CUL4A and -B. We have previously shown this higher-molecular-weight band to be the neddylated form of CUL4 (91). Neddylation is required to activate cullin ubiquitin ligases and is also necessary for Vpr and Vpx functions through CRL4 (91, 94, 95). To test whether the single, slower-migrating band detected in the nucleus is indeed neddylated CUL4, we treated HEK293T cells with the neddylation inhibitor MLN4924 before subcellular fractionation. We subsequently probed for CUL4A or CUL4B and, as expected, observed a shift of nuclear CUL4 in the MLN4924-treated cells to a faster-migrating band (Fig. 7B). Thus, nuclear CUL4A and CUL4B are predominately in the active form. In differentiated primary hMDMs, the intracellular distribution of CUL4A and CUL4B differed from that observed for HEK293T cells or primary T cells. In hMDMs, the CUL4 types were more segregated. CUL4A was mostly cytoplasmic, while CUL4B was mostly nuclear (Fig. 7A, right). In HEK293T cells, primary T cells, and primary hMDMs, SAMHD1 was abundant in the cytoplasm. Nuclear SAMHD1 was most readily detected in hMDMs. Of note, UNG2 was not detectable in hMDMs by Western blotting. This is consistent with the terminally differentiated, noncycling nature of these cells (Fig. 7C) (96, 97). These data indicate that, depending on the cell type or proliferation status, the two CUL4 types are not necessarily segregated into separate compartments.

DISCUSSION

The work presented here demonstrates that while CUL4A and CUL4B have different biological roles, they are interchangeable for HIV Vpr and Vpx functions. HIV-1 Vpr and HIV-2/SIV Vpr can act in the absence of CUL4A or CUL4B, but not both, to trigger G_2 cell cycle arrest. HIV-1 Vpr can utilize either CUL4 type to mediate UNG2 degradation, and for HIV-2 Vpx, the two CUL4 types are interchangeable for SAMHD1 degradation.

Since the initial observation that HIV-1 Vpr was coisolated with CUL4A, the concept that Vpr and Vpx assemble with, and act exclusively through, CUL4A-containing CRL4 complexes has been propagated in numerous studies. Whether Vpr and Vpx act through CUL4A- or CUL4B-containing CRL4 complexes has not been investigated until now. In this work, we demonstrate that Vpr or Vpx can utilize either CUL4A or CUL4B to promote CRL4-dependent functions. These findings extend our understanding of the relationship between the CRL4 complex and HIV and highlight the importance of both CUL4 types in Vpr or Vpx function.

While CUL4A and CUL4B exhibit interchangeability for the Vpr and Vpx functions studied here, they demonstrate unique roles for a number of normal cellular functions. The small yet distinct sequence differences between the two CUL4 types argue against perfect functional redundancy. Indeed, the sequence similarity of the two CUL4 proteins is not always sufficient for functional redundancy, as highlighted by the distinct pathologies associated with CUL4A and CUL4B dysregulation. Whereas CUL4A expression levels are notably elevated in several cancers (58–60) and may impact spermatogenesis (52), CUL4B is critical for normal neuronal development (53–57).

CUL4B is structurally distinguished from CUL4A primarily by an extended amino terminus containing a nuclear localization signal (51). Differences between the subcellular distributions of CUL4B and CUL4A may determine the specificity of their roles in normal cellular biology. CUL4B could transit to the nucleus to fulfill specific CUL4 requirements while CUL4A remains in the cytosol to fulfill other functions. This may be especially important in nondividing cells, like terminally differentiated macrophages. While intracellular location could confer functional specificity, the NLS of CUL4B constitutes a relatively small part of the extended amino terminus. Thus, it is also possible that CUL4B and CUL4A exhibit different structural conformations that allow for the engagement of unique sets of molecular partners. Finally, while we have never seen the expression of only a single CUL4 type in unmanipulated HEK293T cells, primary T cells, or primary hMDMs, we cannot rule out that the two CUL4 forms are differentially regulated in this manner *in vivo*, especially since they are transcribed independently from different chromosomes.

The reported differences between CUL4A and CUL4B led us to hypothesize that Vpr-mediated G_2 cell cycle arrest relies heavily, if not exclusively, on NLS-containing CUL4B. This hypothesis was based on work linking Vpr-triggered G_2 arrest to nuclear events. In both HEK293T cells and primary T cells, we found both CUL4 forms to be abundant in the cytosol. Interestingly, both CUL4 types were also detected in the nucleus in a predominately neddylated, and therefore presumably more active, form. We hypothe-

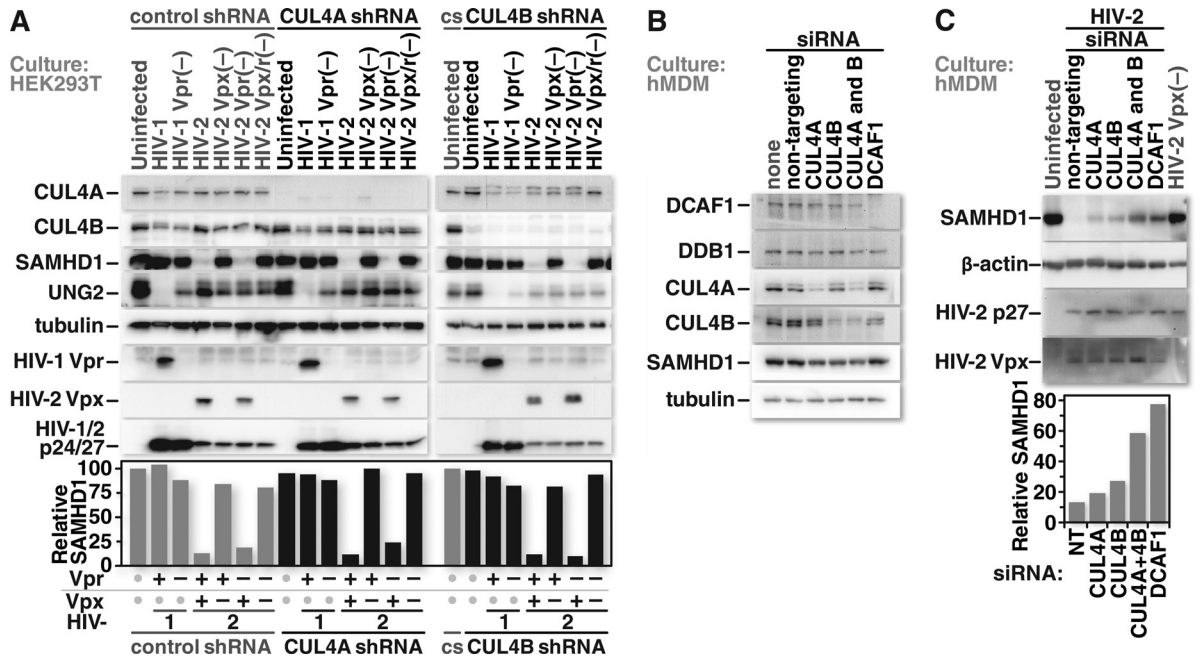

FIG 6 Vpx can initiate SAMHD1 depletion through either CUL4A- or CUL4B-containing CRL4 complexes, but both CUL4 types are required for maximal SAMHD1 depletion in primary macrophages. (A) HEK293T cells that stably express a control shRNA or shRNAs specific for CUL4A or CUL4B mRNAs were either mock infected or infected at equivalent MOIs with HIV-1, HIV-1 lacking Vpr, HIV-2, or HIV-2 lacking Vpr, Vpx, or both. Twenty-four hours after infection, the cells were collected and lysed. Proteins from the whole-cell lysates were resolved by SDS-PAGE and identified by Western blotting using protein-specific antibodies. (B) Cultures of primary human monocyte-derived macrophages (hMDMs) were either mock transfected or transfected with nontargeting siRNA or siRNA specific for the mRNA of the CRL4 complex components indicated. Protein depletion was confirmed by Western blotting. (C, top) Forty-eight hours after siRNA transfection, the cells were either mock infected or infected at a high MOI (MOI = 10) with HIV-2 or HIV-2 lacking Vpx. Less than 24 h after infection, the cells were harvested and lysed. Proteins from whole-cell lysates were resolved by SDS-PAGE and identified by Western blotting with protein-specific antibodies. (Bottom) Densitometric measurements performed on the SAMHD1 bands were normalized to the values of the respective β-actin bands. The relative intensities of the SAMHD1 bands were graphed based on the values obtained from the densitometric analysis. Data shown are representative of a trend observed for samples from 3 different donors.

size that the nearly identical distribution patterns for CUL4A and CUL4B are the reason for their functional interchangeability in this scenario.

In addition to cell cycle arrest and UNG2 depletion, new HIV-1 Vpr phenotypes are being identified. HIV-1 Vpr induces NK cell ligand expression on the surface of infected cells (98–100) as well as the depletion of the endoribonuclease Dicer (101, 102). Both of these phenotypes require the function of the CRL4 complex. Future work investigating the role of CUL4A or CUL4B in these phenotypes will shed additional light on these novel HIV-1 Vpr functions.

The observation that Vpx-mediated SAMHD1 degradation can proceed with CUL4A or CUL4B is particularly interesting because of conflicting reports regarding the subcellular location of SAMHD1 degradation by Vpx. SAMHD1 has a nuclear localization signal at its amino terminus (68, 69, 103). Several laboratories demonstrated that the removal of the NLS, by truncation or mutagenesis, caused the accumulation of SAMHD1 in the cytosol. Importantly, cytoplasmic SAMHD1 was protected from Vpx-mediated degradation despite retaining the capacity to assemble with Vpx (67–69). Furthermore, the steady-state level of NLS-deficient SAMHD1 was found be higher than that of its wild-type counterpart (68). These findings contributed to conclusions that SAMHD1 degradation occurs in the nucleus. Other work led to the conclusion that Vpx brings SAMHD1 from the nucleus into the cytosol to promote its destruction (104). This inference was made because treatment of cells with leptomycin B, an inhibitor of nuclear export, reduced Vpx-mediated SAMHD1 degradation. The demonstration that a Vpx allele that cannot enter the nucleus still promoted SAMHD1 degradation further supported a model in which SAMHD1 is degraded in the cytosol (69, 104). Our work identified CUL4B as the predominant CUL4 type in primary macrophage nuclei. Thus, if SAMHD1 degradation was exclusive to the nucleus, CUL4B depletion should have had the greatest impact on the levels of SAMHD1 in the presence of Vpx. This was not the case. In primary hMDMs, the depletion of neither CUL4A nor CUL4B alone was sufficient to maximally block SAMHD1 degradation by Vpx. Only when both CUL4A and CUL4B were simultaneously depleted was Vpx-mediated SAMHD1 degradation maximally blocked. Furthermore, in hMDMs, SAMDH1 was readily detected in both the cytoplasm and the nucleus. For primary hMDMs, the pattern of SAMHD1 depletion by Vpx (Fig. 6C) and the intracellular distribution of CUL4A, CUL4B, and SAMHD1 (Fig. 7A) complement each other well. Indeed, CUL4A or CUL4B depletion alone only partially rescued SAMHD1 from Vpx-mediated depletion. Given these data, we propose a model in which packaged Vpx utilizes CUL4A in the cytoplasm to enable SAMHD1 degradation there and utilizes CUL4B in the nucleus to enable nuclear SAMHD1 degradation. In this scenario, CUL4A and CUL4B are not fully exchangeable due to their differences in subcellular distribution. Future work validating this model may also help to resolve the discrepancies with regard to SAMHD1

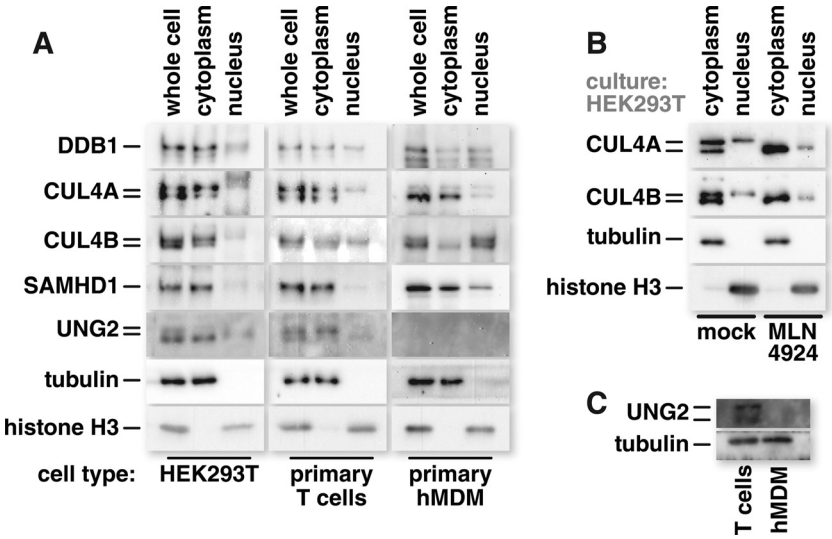

FIG 7 Intracellular CUL4A and CUL4B distributions can vary by cell type. (A) Cultures of HEK293T cells, primary T cells, and primary hMDMs were separated into cytosolic and nuclear fractions by cell membrane lysis and centrifugation of nuclei through a sucrose cushion. Proteins present in the cytosolic or nuclear fraction were resolved by SDS-PAGE and identified by Western blotting using antibodies with the indicated specificities. Tubulin and histone signals were used to confirm the purity of cytosolic and nuclear fractions, respectively, and sample loading was normalized to the signal from whole-cell lysates to ensure an equal representation of cytoplasmic and nuclear lysates. (B) HEK293T cells were pretreated with 1 μM the neddylation inhibitor MLN4924 for 24 h before the cells were harvested and cytosolic and nuclear fractions were isolated. Proteins from cellular fractions were resolved by SDS-PAGE and identified by Western blotting probing for CUL4A, CUL4B, tubulin, and histone. (C) Proteins from the whole-cell lysates of primary T cells and primary hMDMs were resolved by SDS-PAGE, and the levels of tubulin and endogenous UNG2 were assessed by Western blotting. Data shown are representative of a trend observed for 2 different donors.

depletion. Regardless of where SAMHD1 depletion occurs, the data presented in this work demonstrate that either CUL4 type can enable Vpx-mediated SAMHD1 degradation.

Interestingly, we did not observe SAMHD1 to be exclusively nuclear, as reported in a number of studies relying on immunofluorescence. Our observations are most consistent with those of Baldauf et al., who used both 3-dimensional imaging and subcellular fractionation of resting and activated T cells and of macrophages to show that SAMHD1 can be found in both the nucleus and cytoplasm (105). Of course, it is also possible that the intracellular distribution of SAMHD1 varies among cell types and with proliferation status.

Finally, our coimmunoprecipitation experiments showed that CUL4A and CUL4B associate with Vpr and Vpx at different levels. Although both CUL4 types were readily detected after immunoprecipitation of Vpr or Vpx, CUL4A was the predominant species coisolated with Vpr, while more CUL4B was coisolated with Vpx. This difference was surprising because it was not reflected in the CRL4-dependent Vpr and Vpx phenotypes tested here. Interestingly, despite the efficient coisolation of CUL4B, Vpx was coisolated with DCAF1 and DDB1 less efficiently than Vpr. DCAF1 is required for Vpr and Vpx actions through CRL4; however, it is not clear whether all Vpx functions require DCAF1 (106, 107). Specifically, Vpx rescues HIV-1 from an interferon-induced state using a mechanism that is independent of both DCAF1 and dNTP concentrations. It is not known whether the rest of the CRL4 complex is important for this Vpx function. It is also possible that CUL4A and CUL4B have different affinities for, or opportunities to interact with, DDB1. In work to identify cellular partners for cullin proteins, Bennett and colleagues found that proportionally more DDB1 copurified with CUL4A than with CUL4B (108). That work also showed that both CUL4 types associate with numerous WD domain-containing adaptors that could potentially associate with Vpr or Vpx to enable DCAF1-independent access to CRL4.

ACKNOWLEDGMENTS

We thank Karen Duus and Thomas Friedrich for reagents and insightful discussions.

This work was supported by a grant to C.M.C.D.N. from the National Institutes of Health (R01AI073178).

We declare that we have no conflicts of interest.

C.M.C.D.N., H.J.S., and A.K.M.F. conceived of and designed the experiments. H.J.S., A.K.M.F., and R.M.J. performed experiments. C.M.C.D.N. and H.J.S. wrote the manuscript. A.K.M.F., M.D.N., and R.M.J. revised the manuscript. All authors read and approved the final manuscript.

REFERENCES

1. **Yu X, Yu Y, Liu B, Luo K, Kong W, Mao P, Yu XF.** 2003. Induction of APOBEC3G ubiquitination and degradation by an HIV-1 Vif-Cul5-SCF complex. Science **302:**1056–1060. http://dx.doi.org/10.1126/science.1089591.
2. **Stopak K, de Noronha C, Yonemoto W, Greene WC.** 2003. HIV-1 Vif blocks the antiviral activity of APOBEC3G by impairing both its translation and intracellular stability. Mol. Cell **12:**591–601. http://dx.doi.org/10.1016/S1097-2765(03)00353-8.
3. **Sheehy AM, Gaddis NC, Malim MH.** 2003. The antiretroviral enzyme APOBEC3G is degraded by the proteasome in response to HIV-1 Vif. Nat. Med. **9:**1404–1407. http://dx.doi.org/10.1038/nm945.
4. **Marin M, Rose KM, Kozak SL, Kabat D.** 2003. HIV-1 Vif protein binds the editing enzyme APOBEC3G and induces its degradation. Nat. Med. **9:**1398–1403. http://dx.doi.org/10.1038/nm946.
5. **Conticello SG, Harris RS, Neuberger MS.** 2003. The Vif protein of HIV triggers degradation of the human antiretroviral DNA deaminase APOBEC3G. Curr. Biol. **13:**2009–2013. http://dx.doi.org/10.1016/j.cub.2003.10.034.
6. **Mehle A, Strack B, Ancuta P, Zhang C, McPike M, Gabuzda D.** 2004. Vif overcomes the innate antiviral activity of APOBEC3G by promoting

its degradation in the ubiquitin-proteasome pathway. J. Biol. Chem. **279:** 7792–7798. http://dx.doi.org/10.1074/jbc.M313093200.

7. **Mbisa JL, Barr R, Thomas JA, Vandegraaff N, Dorweiler IJ, Svarovskaia ES, Brown WL, Mansky LM, Gorelick RJ, Harris RS, Engelman A, Pathak VK.** 2007. Human immunodeficiency virus type 1 cDNAs produced in the presence of APOBEC3G exhibit defects in plus-strand DNA transfer and integration. J. Virol. **81:**7099–7110. http://dx.doi.org/10.1128/JVI.00272-07.
8. **Chiu YL, Soros VB, Kreisberg JF, Stopak K, Yonemoto W, Greene WC.** 2005. Cellular APOBEC3G restricts HIV-1 infection in resting CD4+ T cells. Nature **435:**108–114. http://dx.doi.org/10.1038/nature03493.
9. **Bishop KN, Holmes RK, Sheehy AM, Davidson NO, Cho SJ, Malim MH.** 2004. Cytidine deamination of retroviral DNA by diverse APOBEC proteins. Curr. Biol. **14:**1392–1396. http://dx.doi.org/10.1016/j.cub.2004.06.057.
10. **Zhang H, Yang B, Pomerantz RJ, Zhang C, Arunachalam SC, Gao L.** 2003. The cytidine deaminase CEM15 induces hypermutation in newly synthesized HIV-1 DNA. Nature **424:**94–98. http://dx.doi.org/10.1038/nature01707.
11. **Mangeat B, Turelli P, Caron G, Friedli M, Perrin L, Trono D.** 2003. Broad antiretroviral defence by human APOBEC3G through lethal editing of nascent reverse transcripts. Nature **424:**99–103. http://dx.doi.org/10.1038/nature01709.
12. **Harris RS, Bishop KN, Sheehy AM, Craig HM, Petersen-Mahrt SK, Watt IN, Neuberger MS, Malim MH.** 2003. DNA deamination mediates innate immunity to retroviral infection. Cell **113:**803–809. http://dx.doi.org/10.1016/S0092-8674(03)00423-9.
13. **Mangeat B, Gers-Huber G, Lehmann M, Zufferey M, Luban J, Piguet V.** 2009. HIV-1 Vpu neutralizes the antiviral factor Tetherin/BST-2 by binding it and directing its beta-TrCP2-dependent degradation. PLoS Pathog. **5:**e1000574. http://dx.doi.org/10.1371/journal.ppat.1000574.
14. **Goffinet C, Allespach I, Homann S, Tervo HM, Habermann A, Rupp D, Oberbremer L, Kern C, Tibroni N, Welsch S, Krijnse-Locker J, Banting G, Krausslich HG, Fackler OT, Keppler OT.** 2009. HIV-1 antagonism of CD317 is species specific and involves Vpu-mediated proteasomal degradation of the restriction factor. Cell Host Microbe **5:**285–297. http://dx.doi.org/10.1016/j.chom.2009.01.009.
15. **Mitchell RS, Katsura C, Skasko MA, Fitzpatrick K, Lau D, Ruiz A, Stephens EB, Margottin-Goguet F, Benarous R, Guatelli JC.** 2009. Vpu antagonizes BST-2-mediated restriction of HIV-1 release via beta-TrCP and endo-lysosomal trafficking. PLoS Pathog. **5:**e1000450. http://dx.doi.org/10.1371/journal.ppat.1000450.
16. **Gupta RK, Hue S, Schaller T, Verschoor E, Pillay D, Towers GJ.** 2009. Mutation of a single residue renders human tetherin resistant to HIV-1 Vpu-mediated depletion. PLoS Pathog. **5:**e1000443. http://dx.doi.org/10.1371/journal.ppat.1000443.
17. **Van Damme N, Goff D, Katsura C, Jorgenson RL, Mitchell R, Johnson MC, Stephens EB, Guatelli J.** 2008. The interferon-induced protein BST-2 restricts HIV-1 release and is downregulated from the cell surface by the viral Vpu protein. Cell Host Microbe **3:**245–252. http://dx.doi.org/10.1016/j.chom.2008.03.001.
18. **Neil SJ, Zang T, Bieniasz PD.** 2008. Tetherin inhibits retrovirus release and is antagonized by HIV-1 Vpu. Nature **451:**425–430. http://dx.doi.org/10.1038/nature06553.
19. **Goldstone DC, Ennis-Adeniran V, Hedden JJ, Groom HC, Rice GI, Christodoulou E, Walker PA, Kelly G, Haire LF, Yap MW, de Carvalho LP, Stoye JP, Crow YJ, Taylor IA, Webb M.** 2011. HIV-1 restriction factor SAMHD1 is a deoxynucleoside triphosphate triphosphohydrolase. Nature **480:**379–382. http://dx.doi.org/10.1038/nature10623.
20. **Ahn J, Hao C, Yan J, DeLucia M, Mehrens J, Wang C, Gronenborn AM, Skowronski J.** 2012. HIV/simian immunodeficiency virus (SIV) accessory virulence factor Vpx loads the host cell restriction factor SAMHD1 onto the E3 ubiquitin ligase complex CRL4DCAF1. J. Biol. Chem. **287:**12550–12558. http://dx.doi.org/10.1074/jbc.M112.340711.
21. **Laguette N, Sobhian B, Casartelli N, Ringeard M, Chable-Bessia C, Segeral E, Yatim A, Emiliani S, Schwartz O, Benkirane M.** 2011. SAMHD1 is the dendritic- and myeloid-cell-specific HIV-1 restriction factor counteracted by Vpx. Nature **474:**654–657. http://dx.doi.org/10.1038/nature10117.
22. **Hrecka K, Hao C, Gierszewska M, Swanson SK, Kesik-Brodacka M, Srivastava S, Florens L, Washburn MP, Skowronski J.** 2011. Vpx relieves inhibition of HIV-1 infection of macrophages mediated by the SAMHD1 protein. Nature **474:**658–661. http://dx.doi.org/10.1038/nature10195.
23. **Lahouassa H, Daddacha W, Hofmann H, Ayinde D, Logue EC, Dragin L, Bloch N, Maudet C, Bertrand M, Gramberg T, Pancino G, Priet S, Canard B, Laguette N, Benkirane M, Transy C, Landau NR, Kim B, Margottin-Goguet F.** 2012. SAMHD1 restricts the replication of human immunodeficiency virus type 1 by depleting the intracellular pool of deoxynucleoside triphosphates. Nat. Immunol. **13:**223–228. http://dx.doi.org/10.1038/ni.2236.
24. **Elder RT, Yu M, Chen M, Zhu X, Yanagida M, Zhao Y.** 2001. HIV-1 Vpr induces cell cycle G2 arrest in fission yeast (Schizosaccharomyces pombe) through a pathway involving regulatory and catalytic subunits of PP2A and acting on both Wee1 and Cdc25. Virology **287:**359–370. http://dx.doi.org/10.1006/viro.2001.1007.
25. **Gummuluru S, Emerman M.** 1999. Cell cycle- and Vpr-mediated regulation of human immunodeficiency virus type 1 expression in primary and transformed T-cell lines. J. Virol. **73:**5422–5430.
26. **Stivahtis GL, Soares MA, Vodicka MA, Hahn BH, Emerman M.** 1997. Conservation and host specificity of Vpr-mediated cell cycle arrest suggest a fundamental role in primate lentivirus evolution and biology. J. Virol. **71:**4331–4338.
27. **Zhao Y, Cao J, O'Gorman MR, Yu M, Yogev R.** 1996. Effect of human immunodeficiency virus type 1 protein R (vpr) gene expression on basic cellular function of fission yeast Schizosaccharomyces pombe. J. Virol. **70:**5821–5826.
28. **Planelles V, Jowett JB, Li QX, Xie Y, Hahn B, Chen IS.** 1996. Vpr-induced cell cycle arrest is conserved among primate lentiviruses. J. Virol. **70:**2516–2524.
29. **He J, Choe S, Walker R, Di Marzio P, Morgan DO, Landau NR.** 1995. Human immunodeficiency virus type 1 viral protein R (Vpr) arrests cells in the G2 phase of the cell cycle by inhibiting p34cdc2 activity. J. Virol. **69:**6705–6711.
30. **Di Marzio P, Choe S, Ebright M, Knoblauch R, Landau NR.** 1995. Mutational analysis of cell cycle arrest, nuclear localization and virion packaging of human immunodeficiency virus type 1 Vpr. J. Virol. **69:**7909–7916.
31. **Wen X, Duus KM, Friedrich TD, de Noronha CM.** 2007. The HIV1 protein Vpr acts to promote G2 cell cycle arrest by engaging a DDB1 and Cullin4A-containing ubiquitin ligase complex using VprBP/DCAF1 as an adaptor. J. Biol. Chem. **282:**27046–27057. http://dx.doi.org/10.1074/jbc.M703955200.
32. **Tan L, Ehrlich E, Yu XF.** 2007. DDB1 and Cul4A are required for human immunodeficiency virus type 1 Vpr-induced G2 arrest. J. Virol. **81:**10822–10830. http://dx.doi.org/10.1128/JVI.01380-07.
33. **Le Rouzic E, Belaidouni N, Estrabaud E, Morel M, Rain JC, Transy C, Margottin-Goguet F.** 2007. HIV1 Vpr arrests the cell cycle by recruiting DCAF1/VprBP, a receptor of the Cul4-DDB1 ubiquitin ligase. Cell Cycle **6:**182–188. http://dx.doi.org/10.4161/cc.6.2.3732.
34. **Hrecka K, Gierszewska M, Srivastava S, Kozaczkiewicz L, Swanson SK, Florens L, Washburn MP, Skowronski J.** 2007. Lentiviral Vpr usurps Cul4-DDB1[VprBP] E3 ubiquitin ligase to modulate cell cycle. Proc. Natl. Acad. Sci. U. S. A. **104:**11778–11783. http://dx.doi.org/10.1073/pnas.0702102104.
35. **DeHart JL, Zimmerman ES, Ardon O, Monteiro-Filho CM, Arganaraz ER, Planelles V.** 2007. HIV-1 Vpr activates the G2 checkpoint through manipulation of the ubiquitin proteasome system. Virol. J. **4:**57. http://dx.doi.org/10.1186/1743-422X-4-57.
36. **Belzile JP, Duisit G, Rougeau N, Mercier J, Finzi A, Cohen EA.** 2007. HIV-1 Vpr-mediated G2 arrest involves the DDB1-CUL4A(VPRBP) E3 ubiquitin ligase. PLoS Pathog. **3:**e85. http://dx.doi.org/10.1371/journal.ppat.0030085.
37. **Laguette N, Bregnard C, Hue P, Basbous J, Yatim A, Larroque M, Kirchhoff F, Constantinou A, Sobhian B, Benkirane M.** 2014. Premature activation of the SLX4 complex by Vpr promotes G2/M arrest and escape from innate immune sensing. Cell **156:**134–145. http://dx.doi.org/10.1016/j.cell.2013.12.011.
38. **Wen X, Casey Klockow L, Nekorchuk M, Sharifi HJ, de Noronha CM.** 2012. The HIV1 protein Vpr acts to enhance constitutive DCAF1-dependent UNG2 turnover. PLoS One **7:**e30939. http://dx.doi.org/10.1371/journal.pone.0030939.
39. **Schröfelbauer B, Yu Q, Zeitlin SG, Landau NR.** 2005. Human immunodeficiency virus type 1 Vpr induces the degradation of the UNG and

SMUG uracil-DNA glycosylases. J. Virol. **79:**10978–10987. http://dx.doi.org/10.1128/JVI.79.17.10978-10987.2005.
40. **Ahn J, Vu T, Novince Z, Guerrero-Santoro J, Rapic-Otrin V, Gronenborn AM.** 2010. HIV-1 Vpr loads uracil DNA glycosylase-2 onto DCAF1, a substrate recognition subunit of a cullin 4A-ring E3 ubiquitin ligase for proteasome-dependent degradation. J. Biol. Chem. **285:**37333–37341. http://dx.doi.org/10.1074/jbc.M110.133181.
41. **Goh WC, Rogel ME, Kinsey CM, Michael SF, Fultz PN, Nowak MA, Hahn BH, Emerman M.** 1998. HIV-1 Vpr increases viral expression by manipulation of the cell cycle: a mechanism for selection of Vpr in vivo. Nat. Med. **4:**65–71. http://dx.doi.org/10.1038/nm0198-065.
42. **Angers S, Li T, Yi X, MacCoss MJ, Moon RT, Zheng N.** 2006. Molecular architecture and assembly of the DDB1-CUL4A ubiquitin ligase machinery. Nature **443:**590–593. http://dx.doi.org/10.1038/nature05175.
43. **He YJ, McCall CM, Hu J, Zeng Y, Xiong Y.** 2006. DDB1 functions as a linker to recruit receptor WD40 proteins to CUL4-ROC1 ubiquitin ligases. Genes Dev. **20:**2949–2954. http://dx.doi.org/10.1101/gad.1483206.
44. **Higa LA, Banks D, Wu M, Kobayashi R, Sun H, Zhang H.** 2006. L2DTL/CDT2 interacts with the CUL4/DDB1 complex and PCNA and regulates CDT1 proteolysis in response to DNA damage. Cell Cycle **5:**1675–1680. http://dx.doi.org/10.4161/cc.5.15.3149.
45. **Jin J, Arias EE, Chen J, Harper JW, Walter JC.** 2006. A family of diverse Cul4-Ddb1-interacting proteins includes Cdt2, which is required for S phase destruction of the replication factor Cdt1. Mol. Cell **23:**709–721. http://dx.doi.org/10.1016/j.molcel.2006.08.010.
46. **Ahn J, Novince Z, Concel J, Byeon CH, Makhov AM, Byeon IJ, Zhang P, Gronenborn AM.** 2011. The Cullin-RING E3 ubiquitin ligase CRL4-DCAF1 complex dimerizes via a short helical region in DCAF1. Biochemistry **50:**1359–1367. http://dx.doi.org/10.1021/bi101749s.
47. **Casey L, Wen X, de Noronha CM.** 2010. The functions of the HIV1 protein Vpr and its action through the DCAF1.DDB1.Cullin4 ubiquitin ligase. Cytokine **51:**1–9. http://dx.doi.org/10.1016/j.cyto.2010.02.018.
48. **Bergamaschi A, Ayinde D, David A, Le Rouzic E, Morel M, Collin G, Descamps D, Damond F, Brun-Vezinet F, Nisole S, Margottin-Goguet F, Pancino G, Transy C.** 2009. The human immunodeficiency virus type 2 Vpx protein usurps the CUL4A-DDB1 DCAF1 ubiquitin ligase to overcome a postentry block in macrophage infection. J. Virol. **83:**4854–4860. http://dx.doi.org/10.1128/JVI.00187-09.
49. **Srivastava S, Swanson SK, Manel N, Florens L, Washburn MP, Skowronski J.** 2008. Lentiviral Vpx accessory factor targets VprBP/DCAF1 substrate adaptor for cullin 4 E3 ubiquitin ligase to enable macrophage infection. PLoS Pathog. **4:**e1000059. http://dx.doi.org/10.1371/journal.ppat.1000059.
50. **Le Rouzic E, Morel M, Ayinde D, Belaidouni N, Letienne J, Transy C, Margottin-Goguet F.** 2008. Assembly with the Cul4A-DDB1-DCAF1 ubiquitin ligase protects HIV-1 Vpr from proteasomal degradation. J. Biol. Chem. **283:**21686–21692. http://dx.doi.org/10.1074/jbc.M710298200.
51. **Zou Y, Mi J, Cui J, Lu D, Zhang X, Guo C, Gao G, Liu Q, Chen B, Shao C, Gong Y.** 2009. Characterization of nuclear localization signal in the N terminus of CUL4B and its essential role in cyclin E degradation and cell cycle progression. J. Biol. Chem. **284:**33320–33332. http://dx.doi.org/10.1074/jbc.M109.050427.
52. **Yin Y, Lin C, Kim ST, Roig I, Chen H, Liu L, Veith GM, Jin RU, Keeney S, Jasin M, Moley K, Zhou P, Ma L.** 2011. The E3 ubiquitin ligase Cullin 4A regulates meiotic progression in mouse spermatogenesis. Dev. Biol. **356:**51–62. http://dx.doi.org/10.1016/j.ydbio.2011.05.661.
53. **Badura-Stronka M, Jamsheer A, Materna-Kiryluk A, Sowinska A, Kiryluk K, Budny B, Latos-Bielenska A.** 2010. A novel nonsense mutation in CUL4B gene in three brothers with X-linked mental retardation syndrome. Clin. Genet. **77:**141–144. http://dx.doi.org/10.1111/j.1399-0004.2009.01331.x.
54. **Isidor B, Pichon O, Baron S, David A, Le Caignec C.** 2010. Deletion of the CUL4B gene in a boy with mental retardation, minor facial anomalies, short stature, hypogonadism, and ataxia. Am. J. Med. Genet. A **152A:**175–180. http://dx.doi.org/10.1002/ajmg.a.33152.
55. **Tarpey PS, Raymond FL, O'Meara S, Edkins S, Teague J, Butler A, Dicks E, Stevens C, Tofts C, Avis T, Barthorpe S, Buck G, Cole J, Gray K, Halliday K, Harrison R, Hills K, Jenkinson A, Jones D, Menzies A, Mironenko T, Perry J, Raine K, Richardson D, Shepherd R, Small A, Varian J, West S, Widaa S, Mallya U, Moon J, Luo Y, Holder S, Smithson SF, Hurst JA, Clayton-Smith J, Kerr B, Boyle J, Shaw M, Vandeleur L, Rodriguez J, Slaugh R, Easton DF, Wooster R, Bobrow M, Srivastava AK, Stevenson RE, Schwartz CE, Turner G, Gecz J, Futreal PA, Stratton MR, Partington M.** 2007. Mutations in CUL4B, which encodes a ubiquitin E3 ligase subunit, cause an X-linked mental retardation syndrome associated with aggressive outbursts, seizures, relative macrocephaly, central obesity, hypogonadism, pes cavus, and tremor. Am. J. Hum. Genet. **80:**345–352. http://dx.doi.org/10.1086/511134.
56. **Zou Y, Liu Q, Chen B, Zhang X, Guo C, Zhou H, Li J, Gao G, Guo Y, Yan C, Wei J, Shao C, Gong Y.** 2007. Mutation in CUL4B, which encodes a member of cullin-RING ubiquitin ligase complex, causes X-linked mental retardation. Am. J. Hum. Genet. **80:**561–566. http://dx.doi.org/10.1086/512489.
57. **Nakagawa T, Xiong Y.** 2011. X-linked mental retardation gene CUL4B targets ubiquitylation of H3K4 methyltransferase component WDR5 and regulates neuronal gene expression. Mol. Cell **43:**381–391. http://dx.doi.org/10.1016/j.molcel.2011.05.033.
58. **Chen LC, Manjeshwar S, Lu Y, Moore D, Ljung BM, Kuo WL, Dairkee SH, Wernick M, Collins C, Smith HS.** 1998. The human homologue for the Caenorhabditis elegans cul-4 gene is amplified and overexpressed in primary breast cancers. Cancer Res. **58:**3677–3683.
59. **Yasui K, Arii S, Zhao C, Imoto I, Ueda M, Nagai H, Emi M, Inazawa J.** 2002. TFDP1, CUL4A, and CDC16 identified as targets for amplification at 13q34 in hepatocellular carcinomas. Hepatology **35:**1476–1484. http://dx.doi.org/10.1053/jhep.2002.33683.
60. **Hung MS, Mao JH, Xu Z, Yang CT, Yu JS, Harvard C, Lin YC, Bravo DT, Jablons DM, You L.** 2011. Cul4A is an oncogene in malignant pleural mesothelioma. J. Cell. Mol. Med. **15:**350–358. http://dx.doi.org/10.1111/j.1582-4934.2009.00971.x.
61. **Liu L, Lee S, Zhang J, Peters SB, Hannah J, Zhang Y, Yin Y, Koff A, Ma L, Zhou P.** 2009. CUL4A abrogation augments DNA damage response and protection against skin carcinogenesis. Mol. Cell **34:**451–460. http://dx.doi.org/10.1016/j.molcel.2009.04.020.
62. **Zimmerman ES, Sherman MP, Blackett JL, Neidleman JA, Kreis C, Mundt P, Williams SA, Warmerdam M, Kahn J, Hecht FM, Grant RM, de Noronha CM, Weyrich AS, Greene WC, Planelles V.** 2006. Human immunodeficiency virus type 1 Vpr induces DNA replication stress in vitro and in vivo. J. Virol. **80:**10407–10418. http://dx.doi.org/10.1128/JVI.01212-06.
63. **Roshal M, Kim B, Zhu Y, Nghiem P, Planelles V.** 2003. Activation of the ATR-mediated DNA damage response by the HIV-1 viral protein R. J. Biol. Chem. **278:**25879–25886. http://dx.doi.org/10.1074/jbc.M303948200.
64. **Tachiwana H, Shimura M, Nakai-Murakami C, Tokunaga K, Takizawa Y, Sata T, Kurumizaka H, Ishizaka Y.** 2006. HIV-1 Vpr induces DNA double-strand breaks. Cancer Res. **66:**627–631. http://dx.doi.org/10.1158/0008-5472.CAN-05-3144.
65. **de Noronha CM, Sherman MP, Lin HW, Cavrois MV, Moir RD, Goldman RD, Greene WC.** 2001. Dynamic disruptions in nuclear envelope architecture and integrity induced by HIV-1 Vpr. Science **294:**1105–1108. http://dx.doi.org/10.1126/science.1063957.
66. **Moir RD, Spann TP, Herrmann H, Goldman RD.** 2000. Disruption of nuclear lamin organization blocks the elongation phase of DNA replication. J. Cell Biol. **149:**1179–1192. http://dx.doi.org/10.1083/jcb.149.6.1179.
67. **Wei W, Guo H, Han X, Liu X, Zhou X, Zhang W, Yu XF.** 2012. A novel DCAF1-binding motif required for Vpx-mediated degradation of nuclear SAMHD1 and Vpr-induced G2 arrest. Cell. Microbiol. **14:**1745–1756. http://dx.doi.org/10.1111/j.1462-5822.2012.01835.x.
68. **Hofmann H, Logue EC, Bloch N, Daddacha W, Polsky SB, Schultz ML, Kim B, Landau NR.** 2012. The Vpx lentiviral accessory protein targets SAMHD1 for degradation in the nucleus. J. Virol. **86:**12552–12560. http://dx.doi.org/10.1128/JVI.01657-12.
69. **Brandariz-Nunez A, Valle-Casuso JC, White TE, Laguette N, Benkirane M, Brojatsch J, Diaz-Griffero F.** 2012. Role of SAMHD1 nuclear localization in restriction of HIV-1 and SIVmac. Retrovirology **9:**49. http://dx.doi.org/10.1186/1742-4690-9-49.
70. **Morner A, Bjorndal A, Albert J, Kewalramani VN, Littman DR, Inoue R, Thorstensson R, Fenyo EM, Bjorling E.** 1999. Primary human immunodeficiency virus type 2 (HIV-2) isolates, like HIV-1 isolates, frequently use CCR5 but show promiscuity in coreceptor usage. J. Virol. **73:**2343–2349.
71. **Schreiber E, Matthias P, Muller MM, Schaffner W.** 1989. Rapid detec-

tion of octamer binding proteins with 'mini-extracts', prepared from a small number of cells. Nucleic Acids Res. **17:**6419. http://dx.doi.org/10.1093/nar/17.15.6419.
72. **Chesebro B, Wehrly K, Nishio J, Perryman S.** 1992. Macrophage-tropic human immunodeficiency virus isolates from different patients exhibit unusual V3 envelope sequence homogeneity in comparison with T-cell-tropic isolates: definition of critical amino acids involved in cell tropism. J. Virol. **66:**6547–6554.
73. **Horton R, Spearman P, Ratner L.** 1994. HIV-2 viral protein X association with the GAG p27 capsid protein. Virology **199:**453–457. http://dx.doi.org/10.1006/viro.1994.1144.
74. **Akkina RK, Walton RM, Chen ML, Li QX, Planelles V, Chen IS.** 1996. High-efficiency gene transfer into CD34+ cells with a human immunodeficiency virus type 1-based retroviral vector pseudotyped with vesicular stomatitis virus envelope glycoprotein G. J. Virol. **70:**2581–2585.
75. **Reil H, Hoxter M, Moosmayer D, Pauli G, Hauser H.** 1994. CD4 expressing human 293 cells as a tool for studies in HIV-1 replication: the efficiency of translational frameshifting is not altered by HIV-1 infection. Virology **205:**371–375. http://dx.doi.org/10.1006/viro.1994.1655.
76. **Balliet JW, Kolson DL, Eiger G, Kim FM, McGann KA, Srinivasan A, Collman R.** 1994. Distinct effects in primary macrophages and lymphocytes of the human immunodeficiency virus type 1 accessory genes vpr, vpu, and nef: mutational analysis of a primary HIV-1 isolate. Virology **200:**623–631. http://dx.doi.org/10.1006/viro.1994.1225.
77. **Connor RI, Chen BK, Choe S, Landau NR.** 1995. Vpr is required for efficient replication of human immunodeficiency virus type-1 in mononuclear phagocytes. Virology **206:**935–944. http://dx.doi.org/10.1006/viro.1995.1016.
78. **Zou Y, Mi J, Wang W, Lu J, Zhao W, Liu Z, Hu H, Yang Y, Gao X, Jiang B, Shao C, Gong Y.** 2013. CUL4B promotes replication licensing by up-regulating the CDK2-CDC6 cascade. J. Cell Biol. **200:**743–756. http://dx.doi.org/10.1083/jcb.201206065.
79. **Kewalramani VN, Park CS, Gallombardo PA, Emerman M.** 1996. Protein stability influences human immunodeficiency virus type 2 Vpr virion incorporation and cell cycle effect. Virology **218:**326–334. http://dx.doi.org/10.1006/viro.1996.0201.
80. **Selig L, Benichou S, Rogel ME, Wu LI, Vodicka MA, Sire J, Benarous R, Emerman M.** 1997. Uracil DNA glycosylase specifically interacts with Vpr of both human immunodeficiency virus type 1 and simian immunodeficiency virus of sooty mangabeys, but binding does not correlate with cell cycle arrest. J. Virol. **71:**4842–4846.
81. **Langevin C, Maidou-Peindara P, Aas PA, Jacquot G, Otterlei M, Slupphaug G, Benichou S.** 2009. Human immunodeficiency virus type 1 Vpr modulates cellular expression of UNG2 via a negative transcriptional effect. J. Virol. **83:**10256–10263. http://dx.doi.org/10.1128/JVI.02654-08.
82. **Priet S, Gros N, Navarro JM, Boretto J, Canard B, Querat G, Sire J.** 2005. HIV-1-associated uracil DNA glycosylase activity controls dUTP misincorporation in viral DNA and is essential to the HIV-1 life cycle. Mol. Cell **17:**479–490. http://dx.doi.org/10.1016/j.molcel.2005.01.016.
83. **Jones KL, Roche M, Gantier MP, Begum NA, Honjo T, Caradonna S, Williams BR, Mak J.** 2010. X4 and R5 HIV-1 have distinct post-entry requirements for uracil DNA glycosylase during infection of primary cells. J. Biol. Chem. **285:**18603–18614. http://dx.doi.org/10.1074/jbc.M109.090126.
84. **Fenard D, Houzet L, Bernard E, Tupin A, Brun S, Mougel M, Devaux C, Chazal N, Briant L.** 2009. Uracil DNA glycosylase 2 negatively regulates HIV-1 LTR transcription. Nucleic Acids Res. **37:**6008–6018. http://dx.doi.org/10.1093/nar/gkp673.
85. **Weil AF, Ghosh D, Zhou Y, Seiple L, McMahon MA, Spivak AM, Siliciano RF, Stivers JT.** 2013. Uracil DNA glycosylase initiates degradation of HIV-1 cDNA containing misincorporated dUTP and prevents viral integration. Proc. Natl. Acad. Sci. U. S. A. **110:**E448–E457. http://dx.doi.org/10.1073/pnas.1219702110.
86. **Kaiser SM, Emerman M.** 2006. Uracil DNA glycosylase is dispensable for human immunodeficiency virus type 1 replication and does not contribute to the antiviral effects of the cytidine deaminase Apobec3G. J. Virol. **80:**875–882. http://dx.doi.org/10.1128/JVI.80.2.875-882.2006.
87. **Sleigh R, Sharkey M, Newman MA, Hahn B, Stevenson M.** 1998. Differential association of uracil DNA glycosylase with SIVSM Vpr and Vpx proteins. Virology **245:**338–343. http://dx.doi.org/10.1006/viro.1998.9159.
88. **BouHamdan M, Xue Y, Baudat Y, Hu B, Sire J, Pomerantz RJ, Duan LX.** 1998. Diversity of HIV-1 Vpr interactions involves usage of the WXXF motif of host cell proteins. J. Biol. Chem. **273:**8009–8016. http://dx.doi.org/10.1074/jbc.273.14.8009.
89. **Bouhamdan M, Benichou S, Rey F, Navarro JM, Agostini I, Spire B, Camonis J, Slupphaug G, Vigne R, Benarous R, Sire J.** 1996. Human immunodeficiency virus type 1 Vpr protein binds to the uracil DNA glycosylase DNA repair enzyme. J. Virol. **70:**697–704.
90. **Schrofelbauer B, Hakata Y, Landau NR.** 2007. HIV-1 Vpr function is mediated by interaction with the damage-specific DNA-binding protein DDB1. Proc. Natl. Acad. Sci. U. S. A. **104:**4130–4135. http://dx.doi.org/10.1073/pnas.0610167104.
91. **Nekorchuk MD, Sharifi HJ, Furuya AK, Jellinger R, de Noronha CM.** 2013. HIV relies on neddylation for ubiquitin ligase-mediated functions. Retrovirology **10:**138. http://dx.doi.org/10.1186/1742-4690-10-138.
92. **Jin J, Ang XL, Shirogane T, Wade Harper J.** 2005. Identification of substrates for F-box proteins. Methods Enzymol. **399:**287–309. http://dx.doi.org/10.1016/S0076-6879(05)99020-4.
93. **St Gelais C, de Silva S, Amie SM, Coleman CM, Hoy H, Hollenbaugh JA, Kim B, Wu L.** 2012. SAMHD1 restricts HIV-1 infection in dendritic cells (DCs) by dNTP depletion, but its expression in DCs and primary CD4+ T-lymphocytes cannot be upregulated by interferons. Retrovirology **9:**105. http://dx.doi.org/10.1186/1742-4690-9-105.
94. **Hofmann H, Norton TD, Schultz ML, Polsky SB, Sunseri N, Landau NR.** 2013. Inhibition of CUL4A neddylation causes a reversible block to SAMHD1-mediated restriction of HIV-1. J. Virol. **87:**11741–11750. http://dx.doi.org/10.1128/JVI.02002-13.
95. **Wei W, Guo H, Liu X, Zhang H, Qian L, Luo K, Markham RB, Yu XF.** 2014. A first-in-class NAE inhibitor, MLN4924, blocks lentiviral infection in myeloid cells by disrupting neddylation-dependent Vpx-mediated SAMHD1 degradation. J. Virol. **88:**745–751. http://dx.doi.org/10.1128/JVI.02568-13.
96. **Hagen L, Kavli B, Sousa MM, Torseth K, Liabakk NB, Sundheim O, Pena-Diaz J, Otterlei M, Horning O, Jensen ON, Krokan HE, Slupphaug G.** 2008. Cell cycle-specific UNG2 phosphorylations regulate protein turnover, activity and association with RPA. EMBO J. **27:**51–61. http://dx.doi.org/10.1038/sj.emboj.7601958.
97. **Hardeland U, Kunz C, Focke F, Szadkowski M, Schar P.** 2007. Cell cycle regulation as a mechanism for functional separation of the apparently redundant uracil DNA glycosylases TDG and UNG2. Nucleic Acids Res. **35:**3859–3867. http://dx.doi.org/10.1093/nar/gkm337.
98. **Pham TN, Richard J, Gerard FC, Power C, Cohen EA.** 2011. Modulation of NKG2D-mediated cytotoxic functions of natural killer cells by viral protein R (Vpr) from HIV-1 primary isolates. J. Virol. **85:**12254–12261. http://dx.doi.org/10.1128/JVI.05835-11.
99. **Richard J, Sindhu S, Pham TN, Belzile JP, Cohen EA.** 2010. HIV-1 Vpr up-regulates expression of ligands for the activating NKG2D receptor and promotes NK cell-mediated killing. Blood **115:**1354–1363. http://dx.doi.org/10.1182/blood-2009-08-237370.
100. **Ward J, Davis Z, DeHart J, Zimmerman E, Bosque A, Brunetta E, Mavilio D, Planelles V, Barker E.** 2009. HIV-1 Vpr triggers natural killer cell-mediated lysis of infected cells through activation of the ATR-mediated DNA damage response. PLoS Pathog. **5:**e1000613. http://dx.doi.org/10.1371/journal.ppat.1000613.
101. **Coley W, Van Duyne R, Carpio L, Guendel I, Kehn-Hall K, Chevalier S, Narayanan A, Luu T, Lee N, Klase Z, Kashanchi F.** 2010. Absence of DICER in monocytes and its regulation by HIV-1. J. Biol. Chem. **285:**31930–31943. http://dx.doi.org/10.1074/jbc.M110.101709.
102. **Casey Klockow L, Sharifi HJ, Wen X, Flagg M, Furuya AK, Nekorchuk M, de Noronha CM.** 2013. The HIV-1 protein Vpr targets the endoribonuclease Dicer for proteasomal degradation to boost macrophage infection. Virology **444:**191–202. http://dx.doi.org/10.1016/j.virol.2013.06.010.
103. **Guo H, Wei W, Wei Z, Liu X, Evans SL, Yang W, Wang H, Guo Y, Zhao K, Zhou JY, Yu XF.** 2013. Identification of critical regions in human SAMHD1 required for nuclear localization and Vpx-mediated degradation. PLoS One **8:**e66201. http://dx.doi.org/10.1371/journal.pone.0066201.
104. **Laguette N, Rahm N, Sobhian B, Chable-Bessia C, Munch J, Snoeck J, Sauter D, Switzer WM, Heneine W, Kirchhoff F, Delsuc F, Telenti A, Benkirane M.** 2012. Evolutionary and functional analyses of the interaction between the myeloid restriction factor SAMHD1 and the lentiviral Vpx protein. Cell Host Microbe **11:**205–217. http://dx.doi.org/10.1016/j.chom.2012.01.007.

105. **Baldauf HM, Pan X, Erikson E, Schmidt S, Daddacha W, Burggraf M, Schenkova K, Ambiel I, Wabnitz G, Gramberg T, Panitz S, Flory E, Landau NR, Sertel S, Rutsch F, Lasitschka F, Kim B, Konig R, Fackler OT, Keppler OT.** 2012. SAMHD1 restricts HIV-1 infection in resting CD4(+) T cells. Nat. Med. **18:**1682–1687. http://dx.doi.org/10.1038/nm.2964.
106. **Pertel T, Reinhard C, Luban J.** 2011. Vpx rescues HIV-1 transduction of dendritic cells from the antiviral state established by type 1 interferon. Retrovirology **8:**49. http://dx.doi.org/10.1186/1742-4690-8-49.
107. **Reinhard C, Bottinelli D, Kim B, Luban J.** 2014. Vpx rescue of HIV-1 from the antiviral state in mature dendritic cells is independent of the intracellular deoxynucleotide concentration. Retrovirology **11:**12. http://dx.doi.org/10.1186/1742-4690-11-12.
108. **Bennett EJ, Rush J, Gygi SP, Harper JW.** 2010. Dynamics of cullin-RING ubiquitin ligase network revealed by systematic quantitative proteomics. Cell **143:**951–965. http://dx.doi.org/10.1016/j.cell.2010.11.017.